

Dense core vesicle transport and synaptic capture in neurons

**by
Alexandra Vela**

B.Sc., Simon Fraser University, 2016

Thesis Submitted in Partial Fulfillment of the
Requirements for the Degree of
Master of Science

in the
Department of Biological Sciences
Faculty of Science

© Alexandra Vela 2019
SIMON FRASER UNIVERSITY
Summer 2019

Copyright in this work rests with the author. Please ensure that any reproduction or re-use is done in accordance with the relevant national copyright legislation.

Approval

Name: **Alexandra Vela**

Degree: **Master of Science**

Title: **Dense core vesicle transport and synaptic capture in neurons**

Examining Committee: **Chair:** Megan Barker
Lecturer

Michael Silverman
Senior Supervisor
Professor

Julian Guttman
Supervisor
Professor

Damon Poburko
Supervisor
Associate Professor

Nancy Hawkins
Internal Examiner
Associate Professor
Department of Molecular Biology and Biochemistry

Date Defended/Approved: August 1, 2019

Ethics Statement

The author, whose name appears on the title page of this work, has obtained, for the research described in this work, either:

- a. human research ethics approval from the Simon Fraser University Office of Research Ethics

or

- b. advance approval of the animal care protocol from the University Animal Care Committee of Simon Fraser University

or has conducted the research

- c. as a co-investigator, collaborator, or research assistant in a research project approved in advance.

A copy of the approval letter has been filed with the Theses Office of the University Library at the time of submission of this thesis or project.

The original application for approval and letter of approval are filed with the relevant offices. Inquiries may be directed to those authorities.

Simon Fraser University Library
Burnaby, British Columbia, Canada

Update Spring 2016

Abstract

Dense core vesicles (DCVs) transport signalling molecules, such as brain-derived neurotrophic factor (BDNF), to neuronal synapses utilizing the kinesin KIF1A. BDNF is critical for neuronal function, therefore it is important to understand DCV trafficking and synaptic capture. I used live-cell imaging to characterize DCVs carrying fluorescently tagged BDNF in hippocampal neurons to assess how they translocate to presynaptic sites. Transport was processive both anterogradely and retrogradely and DCVs can be captured regardless of the direction in which they are traveling. Next, I studied whether absence of doublecortin-like kinase 1 (DCLK1), a KIF1A motility modulator, allows for DCV capture at synapses. Using super-resolution microscopy, DCLK1 co-localized only with a small fraction of axonal DCVs. Despite low co-localization of DCLK1 and DCVs, DCLK1 was absent from most synapses (64%). These observations suggest that DCLK1 may not regulate DCV transport in axons but may regulate movement of other KIF1A cargo.

Keywords: neurons; axonal transport; dense core vesicles; KIF1A; synapse; DCLK1

*To my family, for their unwavering support,
encouragement and unconditional love.*

Acknowledgements

First, I would like to thank my supervisor Dr. Michael Silverman for all the knowledge and opportunities he provided me with throughout my master's degree. I am grateful for his guidance, support, and patience during my research. I would also like to thank my committee members, Dr. Julian Guttman and Dr. Damon Poburko, for their advice and words of encouragement. I also want to thank my current and former lab mates, Aumbreen, Dominic and Maryam for all their help and friendship. Finally, I am grateful for all the support of my family and friends, both near and far, for their constant encouragement, support, and faith in me.

Table of Contents

Approval.....	ii
Ethics Statement.....	iii
Abstract.....	iv
Dedication.....	v
Acknowledgements.....	vi
Table of Contents.....	vii
List of Tables.....	ix
List of Figures.....	x
List of Acronyms.....	xi
Chapter 1. Introduction.....	1
1.1. Axonal transport: overview and significance.....	2
1.1.1. Microtubule based transport.....	6
1.1.2. Motor proteins and bidirectional transport.....	9
1.2. Dense core vesicles.....	12
1.2.1. DCV bidirectional transported.....	13
1.3. KIF1A.....	16
1.4. MAPs and Axonal Transport.....	18
1.5. DCLK1.....	19
1.6. Synaptic delivery.....	20
1.7. Project overview.....	24
Chapter 2. Materials and Methods.....	26
2.1. Hippocampal cell culture and gene transfection.....	26
2.2. Live Imaging.....	26
2.3. Vesicle movement analysis.....	27
2.4. Immunocytochemistry.....	27
2.5. Image analysis.....	28
2.6. Statistical analysis.....	28
Chapter 3. Results.....	30
3.1. DCV movement down the axon.....	30
3.2. DCV behavior near synaptic sites.....	33
3.3. Presence of DCLK1 at synaptic sites.....	36
Chapter 4. Discussion.....	48
4.1. Summary.....	48
4.2. Regulation of bidirectional DCV movement.....	49
4.3. DCV capture at pre-synaptic sites.....	53
4.4. Regulation of KIF1A movement near capture sites.....	56
4.5. Conclusion and future perspectives.....	60
References.....	63

Appendix A69

List of Tables

Table 3-1:	DCV capture can occur regardless of the direction of vesicle movement in axons	36
Table 3-2:	DCLK1 co-localizes with one third of synaptic sites.....	43
Table 3-3:	DCLK1 is present in one third of synaptic sites.....	45

List of Figures

Figure 1-1:	Intracellular transport of cargoes in neurons.....	3
Figure 1-2:	Differences in structural, post-translational modifications and MAPs between axonal and dendritic microtubules.....	8
Figure 1-3:	Structure of motor proteins involved in cargo trafficking.	9
Figure 1-4:	Bidirectional transport regulation	12
Figure 1-5:	Conveyor belt model for DCV distribution in axons.....	14
Figure 1-6:	KIF1A structure and interaction with vesicles and microtubules	17
Figure 1-7:	Synapse structure and composition.....	21
Figure 1-8:	Steps for vesicle accumulation at synapses	23
Figure 3-1:	DCVs move bidirectionally as they travel down the axons and can undergo reversal events.....	31
Figure 3-2:	DCVs exhibit bidirectional trafficking behaviour.	32
Figure 3-3:	Capture sites in axons.....	34
Figure 3-4:	DCVs can be captured at pre-synaptic sites regardless of their direction of movement.	35
Figure 3-5:	DCLK1 is present in both axons and dendrites.....	37
Figure 3-6:	Visual summary of the potential co-localization outcomes between the different markers and their interpretation.	39
Figure 3-7:	DCLK1 is absent from places where DCVs and SVPs co-localize.	41
Figure 3-8:	DCLK1 is absent from 61% of places with accumulated synapsin and Homer.	43
Figure 3-9:	DCLK1 is absent from 66% of synaptic sites	45
Figure 3-10:	DCLK1 co-localizes with 21% of axonal DCVs.	46
Figure 3-11:	Summary of results obtained from MINER analysis.....	47

List of Acronyms

APP	Amyloid precursor protein
BDNF	Brain derived neurotrophic factor
CPE	Corboxypeptidase E
DCV	Dense core vesicles
DC	Doublecortin domain
DCLK1	Doublecortin-like kinase 1
DCX	Doublecortin protein family
DIV	Days in vitro
EB	End-binding protein
FAT	Fast axonal transport
FHA	Forkhead-associated domain
JNK	c-Jun N-terminal kinase
JIP1	JNK-interacting protein 1
MAP	Microtubule associated protein
MINER	Multi-Image Neighborhood Exploring
NPY	Neuropeptide Y
NN	Near neighbour
PF	Protofilament
PH	Pleckstrin homology
PtdIns(4,5)P2	Phosphatidylinositol 4,5bisphosphate
PTV	Piccolo-Basoon vesicle
RIPA	Recursive ImageJ particle analyzer
ROI	Region of interest
SVP	Synaptic vesicle precursor
Syn	Synaptophysin
Syt-4	Synaptotagmin-4

Chapter 1.

Introduction

Neurons are highly polarized and compartmentalized cells. They typically consist of a cell body with branched, tapered dendrites and a long, thin axon. The cell body encompasses the nucleus, endoplasmic reticulum, and Golgi apparatus and thus serves as the principal site for protein synthesis and post-translational modification (Craig & Banker, 1994). Newly synthesized proteins are packaged into vesicles that leave the Golgi apparatus and depend on motor proteins that utilize microtubule-based transport to reach distal portions of the cell including synaptic sites (Hirokawa and Takemura, 2005). Synapses are sites involved in intercellular communication between either two neurons or between a neuron and an effector cell. Synaptic sites can be found along the length of the axon, as *en passant* boutons, or at axon terminals (Bury and Sabo, 2016). Golgi-derived vesicles play a key role in intercellular communication as they contain architectural proteins required for synapse construction and signaling molecules released at synaptic sites.

Among the different vesicles transported in neurons, dense core vesicles (DCVs) are particularly important as they carry neuropeptides essential for neuronal development, function, and survival (Guzik and Goldstein, 2004). Because secretion of these neuropeptides depends on DCV transport and capture at synapses, it is important to understand DCV behavior during these events. The goal of my thesis was to analyze DCV trafficking patterns and to study the regulation of vesicle capture to ultimately have a better understanding of neuronal function. In this chapter, I will begin by introducing axonal transport and more specifically DCV movement and the motor proteins associated with this vesicle population. I will then present an overview of doublecortin-like kinase 1 (DCLK1), a microtubule associated protein, its potential role in the regulation of KIF1A, the motor responsible for DCV transport, and how it might be involved in synaptogenesis. Finally, I will present an outline of my research objectives and hypothesis.

1.1. Axonal transport: overview and significance

Neurons are complex cells made up of specialized cell domains, such as the soma, the axon, and dendrites. Most organelles are localized in the cell body, therefore, neurons need to actively transport a variety of essential intracellular cargoes towards their target location. Neuronal cargoes can move back and forth between the most distal end of the axon and the cell body relying on a bidirectional transport system (Figure 1-1; Brown, 2003). Intracellular cargoes show two distinct types of behavior as they travel on the axon and their movement can be categorized as either slow or fast axonal transport (FAT). Slow axonal transport involves movement of cytoskeletal and cytosolic proteins, whereas FAT encompasses movement of membrane bound organelles (Roy, 2014). The differences in transport behavior are regulated by different factors such as specific cargo-motor interactions and cargo-microtubule binding. Motor proteins can bind various cargoes and display different movement behaviors depending on the interactions mentioned before. For example, the motor protein KIF5 is known to transport mRNA granules, mitochondria, and also vesicles containing receptors, and it displays different movement behaviors based on the cargo attached. (Hirokawa et al., 2010).

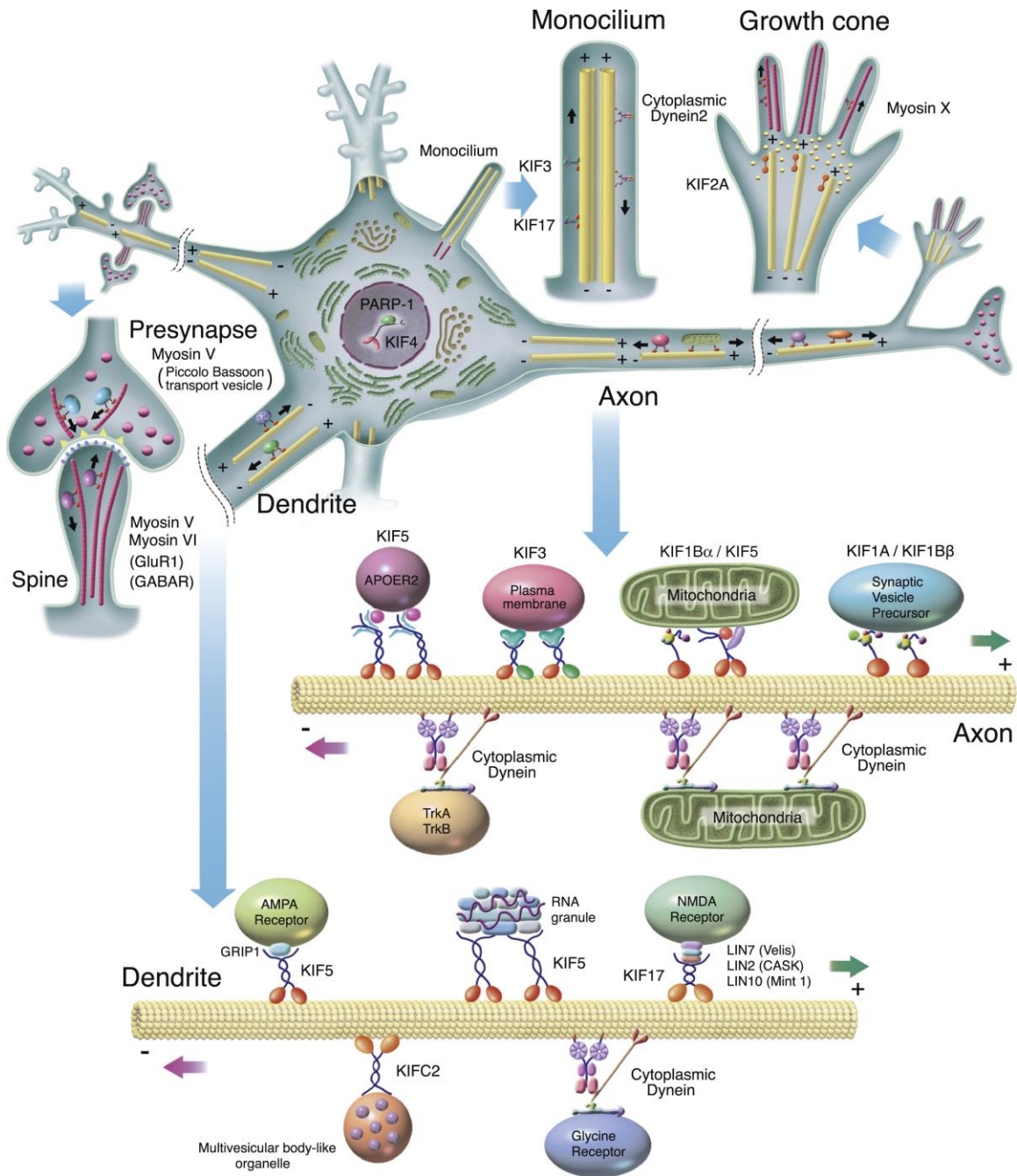


Figure 1-1: Intracellular transport of cargoes in neurons.

Intracellular cargoes in neurons are transported in axons and dendrites by a variety of motor proteins. Kinesin proteins, such as KIF1A and KIF5, are responsible for anterograde transport of organelles. For example, KIF1A and KIF5 transport synaptic vesicle precursors and RNA granules towards the plus-end in axons and dendrites. In contrast, Cytoplasmic dynein is responsible of retrograde transport. Cytoplasmic dynein moves cargo, such as vesicles containing AMPA and Glycine receptors, towards the minus-end of microtubules. Cargoes, such as mitochondria, can bind both motor proteins and move bidirectionally. (Hirokawa et al., 2010)

Non-membranous organelles display the slowest velocities while traveling down the axon, with speeds ranging from 0.01 $\mu\text{m/s}$ for the movement of microtubule subunits to 0.02-0.09 $\mu\text{m/s}$ for microfilaments movement. Although initially it was thought that the low transport rate was the result of slow motor proteins, it has been shown that all motors move at approximately the same speed (Brown, 2003). Instead, cargoes that are part of the slow axonal transport system move with a distinct “stop and go” pattern. This pattern is characterized by infrequent motor movement and short run lengths, which causes an overall slowing of the rate of movement (Roy, 2014).

Unlike slow axonal transport, the movement of cargoes that are part of the FAT system is highly processive. FAT cargoes are transported either embedded in the membrane or in the lumen of organelles and have short and infrequent pauses as they move to their target destination. These organelles can move at speeds ranging from 0.5–2 $\mu\text{m/s}$ and rely on the motor proteins kinesin and dynein, and on dynamic microtubules that act as tracks for motor protein movement (Tang et al., 2013; Maday et al., 2014). An example of FAT vesicles are lysosomes and autophagosomes which move at high speeds, 0.5-1 $\mu\text{m/s}$, as they travel down the axon. Lysosomes and autophagosomes can travel bidirectionally as they are attached to kinesin motors, such as KIF5, and dynein. However, lysosomes have an anterograde bias for movement whereas autophagosomes move mostly in a retrograde direction (Brown, 2003; Klinman & Holzbaur, 2016).

Mitochondria are also part of the same FAT system that includes SVPs and DCVs, even though they do not travel in the same pattern as FAT vesicles do. Mitochondria are transported by KIF5 and dynein and move bidirectionally, but they exhibit a characteristic saltatory pattern of movement. Mitochondrial movement is characterized by frequent pausing, sudden changes in velocity, and reversal events. Despite differences in the number of mitochondria present in axons versus dendrites, they exhibit the same trafficking behavior in both compartments. This observation suggests that it is regulation of cargo drop off that is responsible for the differences in the number of axonal mitochondria compared to dendritic (Ligon and Steward, 2000). Differences in mitochondria localization is an example of how establishment of the different cellular subcompartments depends not only in regulation of motor movement but also in regulations of the motor-cargo interactions.

SVPs and DCVs are vesicles that are also part of the FAT system in neurons. SVPs are small vesicles that transport synaptic vesicle components such as synaptophysin and syntaxin. Components of synaptic vesicles are packaged either in the lumen or embedded in the membrane of SVPs. At synapses, SVP components are used to form synaptic vesicles and therefore, SVPs need to accumulate at synaptic sites. SVPs use KIF1A for anterograde transport and dynein for retrograde transport (Goldstein et al., 2008). The exact protein interactions responsible for cargo binding between SVPs and motor proteins is unclear. However, it is known that the interaction involves the pleckstrin homology (PH) domain part of KIF1A and phosphatidylinositol 4,5bisphosphate (PtdIns(4,5)P₂) present on the SVP membrane (Goldstein et al., 2008).

Along with SVPs, DCVs are large secretory vesicles that are part of the FAT system that accumulate at synaptic sites because they carry neuropeptides and neurotrophins essential for neuron survival and synaptic function. DCVs release their cargo during synaptic activity via vesicle fusion. However, DCVs cannot be recycled after vesicle fusion, therefore, correct neuronal function depends on adequate resupply of these vesicles to synaptic sites following activity (Gondré-Lewis et al., 2012). DCVs also rely on KIF1A and cytoplasmic dynein to move from the soma to pre-synaptic sites and accumulate there waiting for release during activity (Kwinter, et al., 2009).

Regulated cargo trafficking is essential for proper neuronal function as evidenced by the range of neurodegenerative diseases that stem from disruptions in cargo transport. For example, gene mapping studies showed that mutations to the dynein and kinesin loci cause phenotypes observed in neurodegenerative diseases such as Amyotrophic Lateral Sclerosis, Charcot-Marie-Tooth syndrome, and hereditary spastic paraplegia (Yuan et al., 2017). Furthermore, impaired cargo movement caused by damage to the motor protein, faulty motor-cargo binding, damage to the microtubule tracks, or deficiency in ATP supply significantly contribute to the synaptic loss and axonal degeneration observed in Alzheimer's disease (Wang, Tan, & Yu, 2015).

1.1.1. Microtubule based transport

Axon and dendrites are neuronal subcompartments with very distinct compositions established by protein sorting due to selective transport of intracellular cargoes. Studies following fluorescently-tagged membrane proteins showed that there is microtubule-based selective transport of different cargoes into dendrites and axons (Burack et al., 2000). Because cargoes rely on motor proteins for transport, their movement highly depends on cytoskeletal proteins that act as tracks for the motors. Cytoskeletal structures, such as actin and microtubules, are therefore closely associated with the regulation of transport in neurons.

Microtubules are cylinders made of $\alpha\beta$ -tubulin dimers that have a highly dynamic behavior. In axons, the β -tubulin end, or “positive” side, faces the distal end of the axon whereas the α -tubulin end, or “negative” side, is closest to the cell body. Dendrites have microtubules with mixed polarities (Chevalier-Larsen and Holzbaur, 2006). Difference in structural features of microtubules affect vesicle trafficking in neurons. For example, microtubule orientation in axons influence the direction of vesicle movement. Vesicles attached to a kinesin, a positive-end motor protein, move towards the most distal end in axons whereas vesicles moving back towards the cell body are usually attached to dynein, a negative-end motor protein (Nogales & Zhang, 2016). Selective transport in dendrites relies on more than just motor protein activation because dendrites have mixed polarity microtubules.

In addition to polarity, post-translational modifications and microtubule associate proteins (MAPs) affect microtubule structure and therefore also play a role in the regulation of selective transport (Nakata and Hirokawa, 2003; Lipka et al., 2016). Microtubules have specific post-translational modifications depending on the cellular compartment where they are located. For example, axons contain mostly detyrosinated microtubules and are therefore more stable compared to dendritic microtubules, which are not detyrosinated to the same extent. Furthermore, dendrites have a lower ratio of acetylated microtubules than axons, which indicates that microtubules in dendrites are more dynamic (Kapitein & Hoogenraad, 2011). Differences in post-translational modifications in microtubules affect selective transport of motor proteins. For example, high detyrosination levels in axonal microtubules guides selective movement of some kinesins, such as KIF5, into this compartment (Kapitein and Hoogenraad, 2011).

Microtubule structure and selective transport can also be modified by MAPs. MAPs are a large family of proteins that bind to microtubules and can modify microtubule structure, dynamics, and motor protein interactions (Kapitein & Hoogenraad, 2011). An example of MAPs that regulate microtubule structure are the end-binding protein family (EB) which regulate microtubule growth and their sorting to the correct cellular compartment (van Beuningen & Hoogenraad, 2016). Furthermore, other MAPs, such as TRIM 46, can regulate the establishment of microtubule polarity in axons (van Beuningen & Hoogenraad, 2016). MAPs can cause architectural changes in MT structure that affect motor protein binding. Proteins such as tau, MAP2 and DCLK1 are examples of MAPs that can affect vesicle movement in axons and dendrites (Kapitein and Hoogenraad, 2011; Atherton et al., 2013). Differential MAP distribution, along with post-translational microtubule modifications, such as polyglutamylation and detyrosination/tyrosination, all play a role in cargo sorting in neurons by regulating motor protein movement (Figure 1-2).

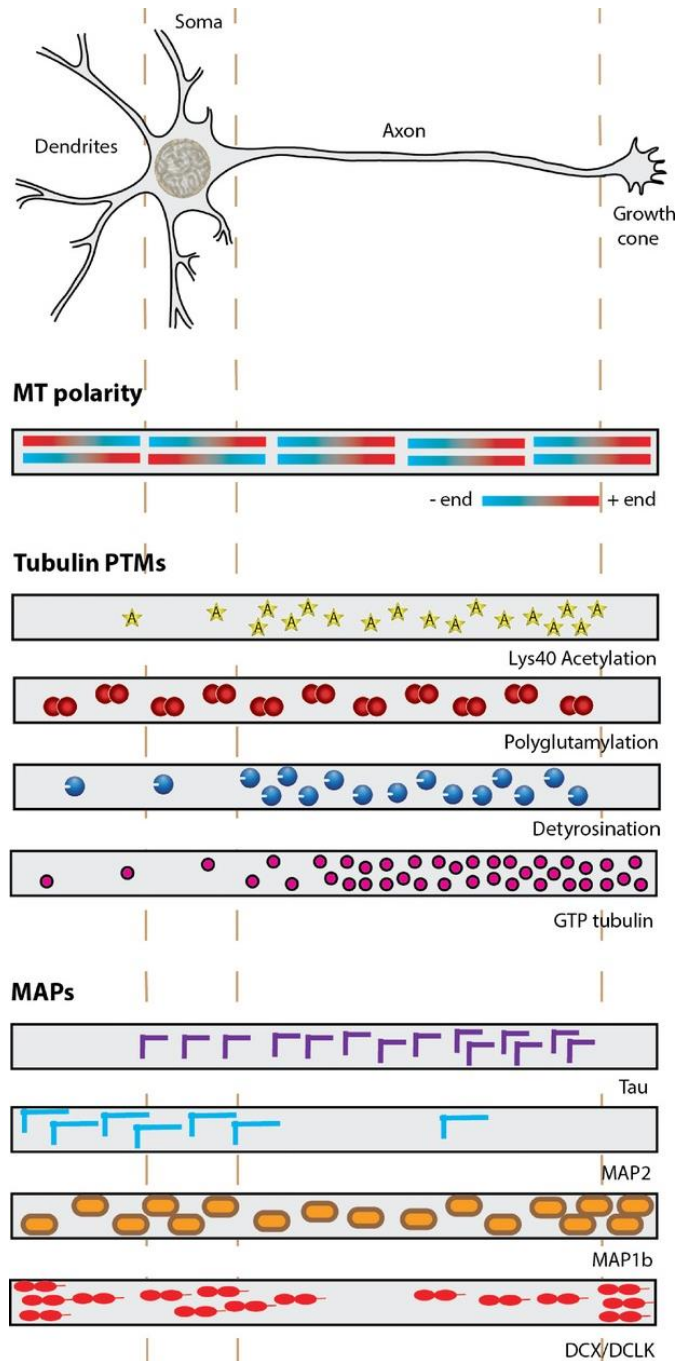


Figure 1-2: Differences in structural, post-translational modifications and MAPs between axonal and dendritic microtubules

Microtubule polarization and structural modifications are different depending on the cellular compartment in which the microtubules are located. All axonal microtubules have the same orientation, all the microtubules plus-end face the distal side. Dendritic microtubules have mixed polarities. Furthermore, axonal and dendritic microtubules have different post-translational modifications. For example, axons have more acetylated and detyrosinated microtubules than dendrites. Distribution of MAPs, such as Tau and MAP2, also varies between axons and dendrites. Tau accumulates in axonal microtubules whereas MAP2 accumulates in dendrites. These differences in microtubule structure help regulate selective motor protein movement in axons and dendrites (Atherton et al., 2013)

1.1.2. Motor proteins and bidirectional transport

Cargo trafficking along the axon depends on microtubule-based transport by kinesin and dynein motors. The kinesin superfamily of motor proteins comprises 45 different members organized in 15 major families. Approximately half of the kinesin family is responsible for intracellular cargo transport while the remaining ones act in cell division (Hirokawa et al., 2009). In contrast, the dynein protein family is far less diverse, but it plays an equally important role in cargo transport. Although kinesin and dynein are different in size, they are both ATP dependent and have specialized domains to interact with the microtubules and the cargo they are transporting (Figure 1-3; Goldstein & Yang, 2000).

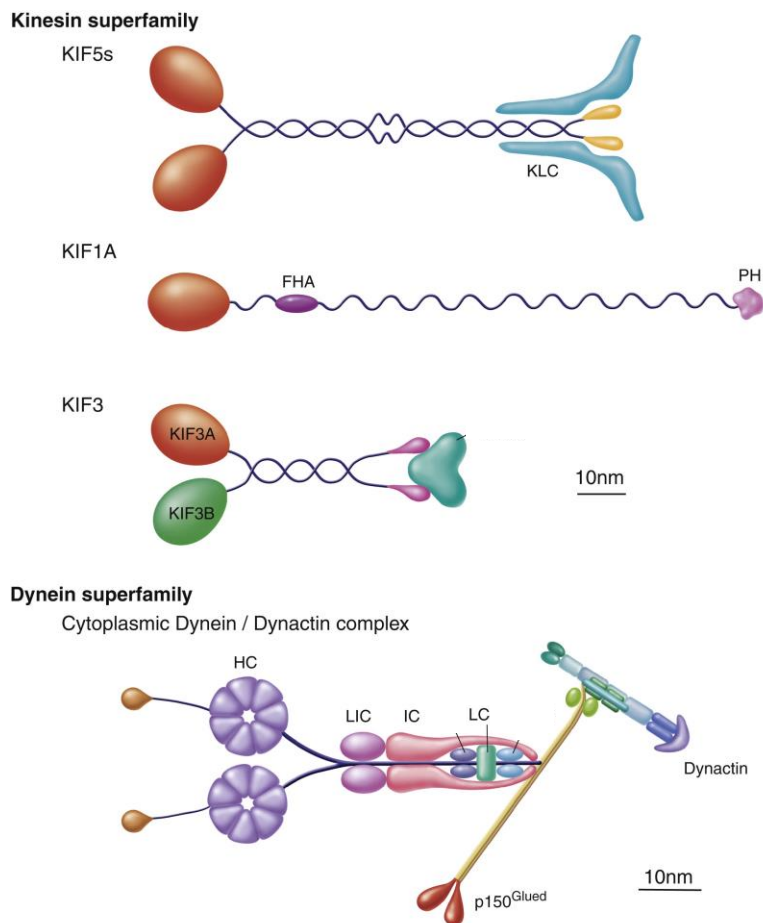


Figure 1-3: Structure of motor proteins involved in cargo trafficking.

Kinesins and cytoplasmic dynein are the motor proteins responsible for axonal transport. Although the structure of kinesins associated with vesicle movement vary from one another, most kinesins have a similar overall structure and move anterogradely. These kinesins have a globular motor domain, a regulatory stalk region, and a cargo binding tail. Cytoplasmic dynein moves cargo in a retrograde direction. Dynein is made of a heavy chain, a light intermediate chain,

intermediate chains, and light chains. Binding to the dynactin complex, via the p150 subunit, is necessary for dynein movement (Hirokawa et al., 2010). KLC= Kinesin light chain; FHA= Forkhead domain; PH= Pleckstrin homology domain; HC= Dynein heavy chain; LIC= Dynein light intermediate chain; IC= Dynein intermediate chain; LC= Dynein light chain

All kinesins have a motor domain, which can be located either at the N-terminal, the middle region, or the C-terminal. Kinesins with a motor domain in the middle region are involved in regulation of microtubule polymerization and cell division. Kinesins with an N-terminal motor are responsible for plus-end transport, while those with a C-terminal motor domain function primarily in negative-end transport (Hirokawa et al., 2009). In addition to a motor domain, they all have a distinct stalk and a tail region. Cargo selectivity in kinesin family members relies on different binding domains in the tail region (Hirokawa et al., 2010a). In addition to cargo binding, the stalk and tail domains also play a role in dimerization of kinesins and thus regulate motor activation. (Goldstein & Yang, 2000).

In contrast to kinesin, the dynein family of proteins is less diverse but with a more complex structure. The dynein family is comprised of two types of motor complexes; cytoplasmic dynein and axonemal dynein. Of the two types of dynein, cytoplasmic dynein acts as a negative-end motor protein for vesicle transport and it moves by hydrolyzing ATP (Hirokawa, 1998). Dyneins are multi-domain proteins made up of a heavy chain, intermediate chains, light intermediate chains, and light chains; interaction between the various domains and associated proteins allows for cargo binding and regulation (Goldstein & Yang, 2000). Specifically, cytoplasmic dynein interacts with the dynactin complex, which includes proteins such as ARP1 and p150, to regulate cargo binding and movement. (Hirokawa & Takemura, 2005). Furthermore, interaction between dynactin, dynein, and kinesins appear to regulate coordinated bidirectional transport (Chen et al., 2019).

Observations of axonal and dendritic movement of different vesicles that are part of the FAT system show that vesicles can move anterogradely and retrogradely. Furthermore, most vesicles can pause and switch directions as they travel on neuronal processes (Maday et al., 2014). These observations raise the question as to what regulates motor protein activation and switches during bidirectional transport. There are several models that could explain regulation of bidirectional transport (Figure 1-4). One model, called selective recruitment, involves regulation of movement by controlling cargo

and motor protein interaction. An example of this model is the regulation of dynein and some kinesin motors, such as KIF5 and KIF1A, by dynactin interaction (Park et al., 2009). Studies in which dynactin was disrupted showed a decrease not only in retrograde but also anterograde movement. Specifically, dynactin seems to regulate bidirectional movement by selectively allowing attachment of either kinesins or dynein motors to the cargo (Gross et al., 2002)

Another mechanism, called the coordination model, suggests that all motor proteins are already attached to the vesicle and that instead, their activation, via multimerization or selective binding to the corresponding cytoskeleton structure, is what regulates the switch between directions. Scaffolding proteins such as Huntingtin and JNK-interacting protein 1 (JIP1) can form complexes with both kinesin and dynein motors and their cargo, and thus serve as examples of proteins that regulate movement in the coordination model (Fu and Holzbaur, 2014). Finally, another possible mechanism of bidirectional transport regulation is the “tug of war” model. In this model, groups of motor proteins of opposite polarity compete against each other until the pull in one of the directions overcomes the opposite one. This model is used to explain how movement of organelles bound to multiple motors, such as endosomes and lysosomes, can be regulated (Maday et al., 2014). The most common mechanism in mammalian neurons is the coordination model and explains movement of most fast-moving cargoes such as autophagosomes, and most Golgi-derived organelles, such as SVPs and DCVs (Maday et al., 2014).

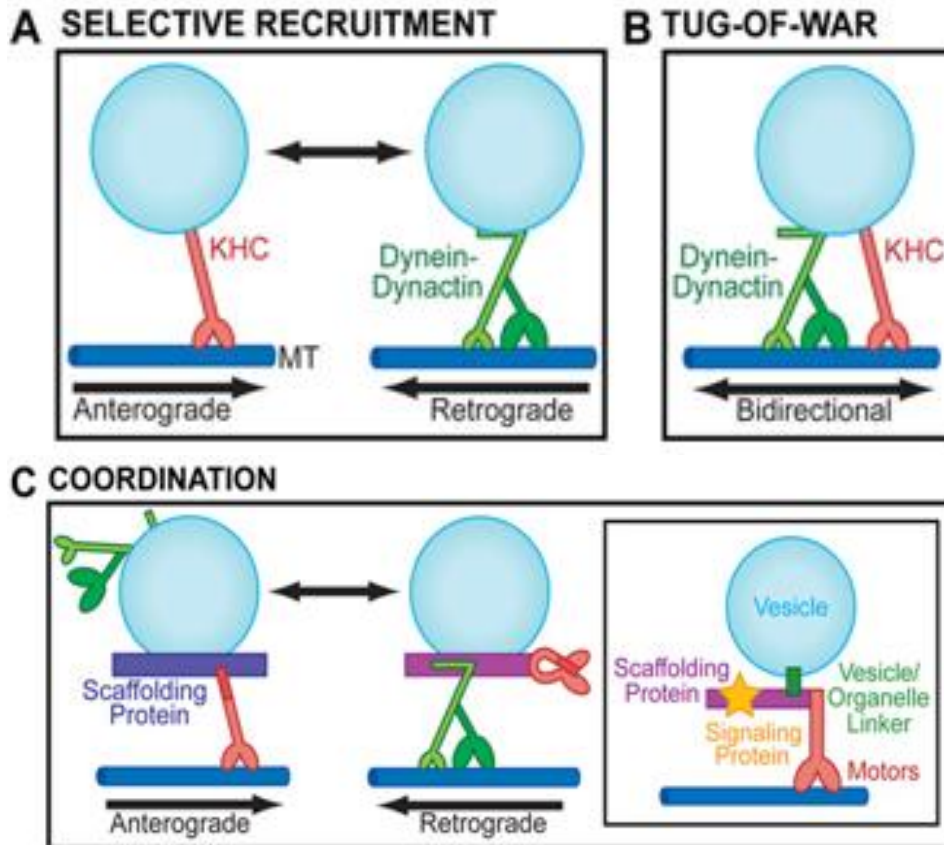


Figure 1-4: Bidirectional transport regulation

Bidirectional transport in neurons can be regulated by different mechanisms. In the Selective recruitment model (A), direction of movement is determined by activation of one motor by selective cargo binding. In contrast, in the tug of war model (B), both motor proteins are already attached, and direction of movement is determined by whichever motor has a stronger pull. Finally, in the coordination model (C), both motors are attached to the vesicle and direction of travel depends on selective activation of only one of them. (Fu and Holzbaaur, 2014).

1.2. Dense core vesicles

DCVs are organelles that deliver signaling molecules to target locations in secretory cells such as neurons and endocrine cells. In neurons, DCVs carry neuropeptides that are synthesized in the cell body and travel long distances towards pre- and post- synaptic sites. After protein synthesis, DCV cargo selection is regulated by chromogranin A and chromogranin B, which promote protein aggregation and sorting into DCVs at the trans Golgi network (Dominguez et al., 2018). DCVs then bud out from the Golgi apparatus as immature vesicles and undergo maturation as they travel to their final destination (Gondré-Lewis et al., 2012). During maturation, DCV cargo is cleaved, missorted proteins are removed, and the lumen of the vesicle is acidified (Cohen & Greenberg, 2008).

A type of essential cargo transported in DCVs are neurotrophins such as brain-derived neurotrophic factor (BDNF; Gondré-Lewis et al., 2012). Like most neurotrophins, BDNF is essential for synapse formation and maintenance, therefore deficiencies in this neuropeptide are related to neurodegenerative disorders (Cohen & Greenberg, 2008). Specifically, deficiencies in BDNF secretion are associated with disorders marked with significant memory loss, such as Alzheimer's, Parkinson's and Huntington's diseases (Numakawa et al., 2018). Furthermore, BDNF plays a role in the regulation of brain inflammation and cell response to a stressor. A decrease in BDNF levels contributes to faster cell death, which emphasizes the importance of adequate neuropeptide delivery for cell survival (Lima Giacobbo et al., 2018).

Another important cargo transported in DCVs is neuropeptide Y (NPY). NPY is important because of its role in neurogenesis and neuroprotection. NPY is a widely expressed neuropeptide in the central nervous system, regulating processes such as feeding, circadian rhythms, and energy homeostasis (Kormos & Gaszner, 2013). Because NPY plays a crucial role in regulating cellular response to stress, a decrease in NPY also leads to physical and behavioral changes often associated with anxiety and depression (Alldredge, 2010).

1.2.1. DCV bidirectional transported

Studies in *C. elegans* demonstrated that UNC-104, a kinesin-3 family member, is required for anterograde transport of DCVs (Barkus, et al., 2008). Further research in our lab showed that KIF1A, a UNC-104 homologue, was the kinesin responsible for anterograde movement of DCVs in mammalian neurons (Lo et al., 2011). Studies of BDNF containing vesicles identified dynactin as having a key role in regulation of motor protein binding. Specifically, carboxypeptidase E, a DCV transmembrane protein, interacts with dynactin to promote motor protein recruitment (Park et al., 2008). Studies in our lab in which dynactin and DCV interaction were altered confirmed its role in vesicle transport not only for dynein-associated retrograde movement but also for anterograde transport (Kwinter et al., 2009).

Studies of DCV movement in *Drosophila* neurons showed that DCVs follow a specific trafficking pattern, as they move towards *en passant* boutons and the axon terminal, to ensure correct vesicle supply to boutons and axon termini (Wong et al.,

2012). Using fluorescence microscopy in *Drosophila* neurons, researchers observed that DCVs move in a “conveyor belt” pattern as they travel bidirectionally along the axon (Figure 1-5). In this pattern, all vesicles enter the proximal axon and move anterogradely towards the axon terminal, bypass the *en passant* boutons and first accumulate at the most distal end. Once enough DCVs are delivered to the terminal, the remaining vesicles switch directions and begin to move back towards the cell body, at which time a small percentage of vesicles are captured at *en passant* boutons. Before the vesicles re-enter the cell body, they switch directions again and once more move anterogradely towards the distal portion of the axon to fill the remaining *en passant* pre-synaptic sites (Moughamian & Holzbaaur, 2012; Wong et al., 2012). Due to the difficulty in vesicle imaging in mammalian neurons, very few studies regarding vesicle trafficking in these cells have been carried out. A recent study detailing DCV trafficking pattern in mammalian neurons found that these vesicles move in both directions, as in the *Drosophila* model, but direction switches can happen at different points in the axon (Bharat et al., 2017).

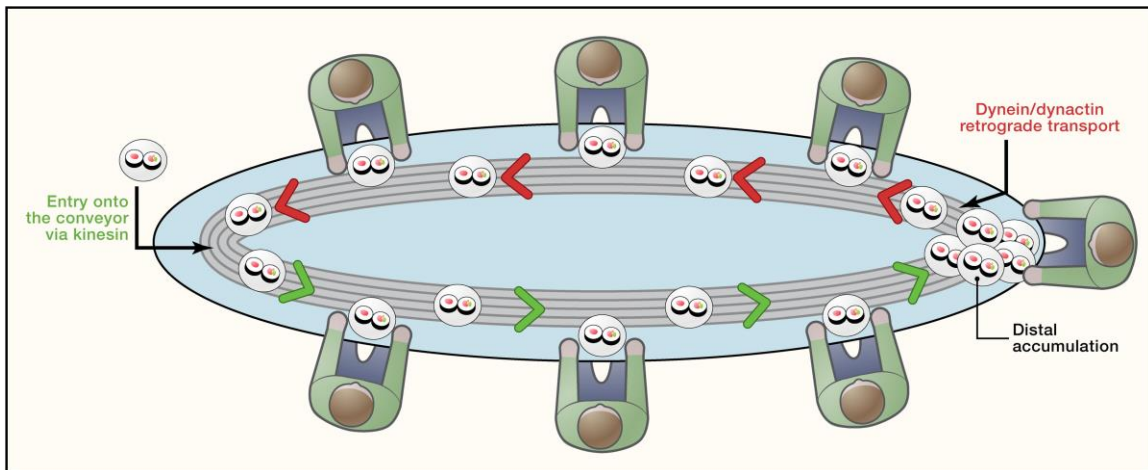


Figure 1-5: Conveyor belt model for DCV distribution in axons.

DCVs follow a specific trafficking pattern while traveling down the axon towards synaptic sites. To fill *en passant* boutons and terminals, DCVs enter the axon and move anterogradely to accumulate at the most distal bouton first. The vesicles not captured at the distal end then switch directions and fill the *en passant* boutons along the axon as they travel retrogradely. Before DCVs re-enter the cell body, they switch directions and move anterogradely once again. This pattern is repeated until all synapses are filled. (Moughamian and Holzbaaur, 2012)

The conveyor belt model explains how DCVs are supplied during initial vesicle accumulation at synapses, but the trafficking pattern following synaptic activity seems to be different. During activity, neuropeptide release occurs via vesicle fusion and therefore

synapses, where release took place, require a resupply of DCVs. Quantification of vesicle trafficking after activity showed an increase in capture in vesicles traveling retrogradely. This switch occurs to ensure adequate DCV resupply to synapses where DCV accumulation is reduced due to activity (Shakiryanova, Tully, & Levitan, 2006). The mechanism by which this transient enhancement of vesicle capture occurs has yet to be understood.

Once DCVs reach synapses, vesicle capture and accumulation are required for neuropeptide release during synapse activity. Although the mechanism that controls vesicle drop off and accumulation at synapses is still unclear, a recent study in mammalian neurons suggests that destabilization of the interaction between KIF1A and DCVs is involved in capture. In this mechanism, modification of the cargo and motor protein interaction causes vesicles to pause at synaptic sites, which could then facilitate vesicle capture and accumulation. Synaptotamgin-4 (syt-4), a protein that aids in KIF1A binding to DCVs, is an example of how this mechanism regulates vesicle capture in mammalian neurons. (Bharat et al., 2017). Furthermore, studies observing KIF1A movement near capture sites showed that microtubule structure, specifically accumulation of microtubule ends at synapses, also regulates vesicle pausing at synaptic sites (Guedes-Dias et al., 2019a).

DCVs accumulate at synapses and undergo exocytosis during activity; however, the mechanism that regulates vesicle fusion for cargo release is still unclear. Studies in *Drosophila* neurons showed that dynamin has a potential role in regulating vesicle fusion, as it triggers partial vesicle fusion and incomplete neuropeptide release from DCVs. Partial release of the DCV contents allow the vesicles to sustain more rounds of activity. These studies also showed that vesicle fusion can occur regardless of whether the vesicle is traveling anterogradely or retrogradely. This suggests that all the DCVs circulating in the axons are mature and ready for neuropeptide release. (Wong, Cavolo, & Levitan, 2015).

Further research in *C. elegans* neurons showed that CaMKII may also regulate vesicle fusion by preventing premature DCV exocytosis in the soma (Hoover et al., 2014; Nurrish, 2014). This study showed that CaMKII mutants had a decrease of DCVs moving in axons and dendrites due to premature vesicle fusion and neuropeptide release. Vesicle tracking studies showed that a reduction in CaMKII did not have an effect on

vesicle movement. Instead, the decrease in moving DCVs was due to premature vesicle fusion in the cell body, before the vesicles entered the axon, and not disruption of transport. Gain-of-function CaMKII mutations inhibit neuropeptide release in axons, thus further proving that CaMKII plays a role in regulating DCVs vesicle fusion. (Hoover et al., 2014; Nurrish, 2014)

1.3. KIF1A

DCVs rely on KIF1A and cytoplasmic dynein for anterograde and retrograde movement respectively (Lo et al., 2011). KIF1A is a brain enriched kinesin responsible for long range transport. It is a highly efficient motor and moves at a speed of $\sim 1.2 \mu\text{m/s}$, one of the faster kinesins, and can have extended run lengths (Okada et al., 1995). Similar to other kinesins, KIF1A has a multi-domain structure consisting of a motor domain (containing the microtubule and ATP binding sequences), as well as a neck, stalk, and tail domain. The motor domain on KIF1A is an anterograde motor localized at the N-terminus of the protein. Although KIF1A has an overall common kinesin structure, it also has several unique features (Hirokawa & Noda, 2008).

Adjacent to the motor domain, KIF1A has a specialized neck region containing a K-loop of lysines. This K-loop increases microtubule binding affinity, which helps enhance motor protein processivity. The forkhead-associated domain (FHA), which has structural and cargo binding functions, is also present in the neck region. Additionally, KIF1A has a pleckstrin homology (PH) domain in the tail region that allows for cargo binding (Figure 1-6). Furthermore, the neck, stalk and tail regions are involved in motor protein activation, as their interaction results in a folded, monomeric, autoinhibited motor protein. Cargo binding releases the motor from its folded state and allows for dimerization via the neck and stalk domains (Siddiqui & Straube, 2017)

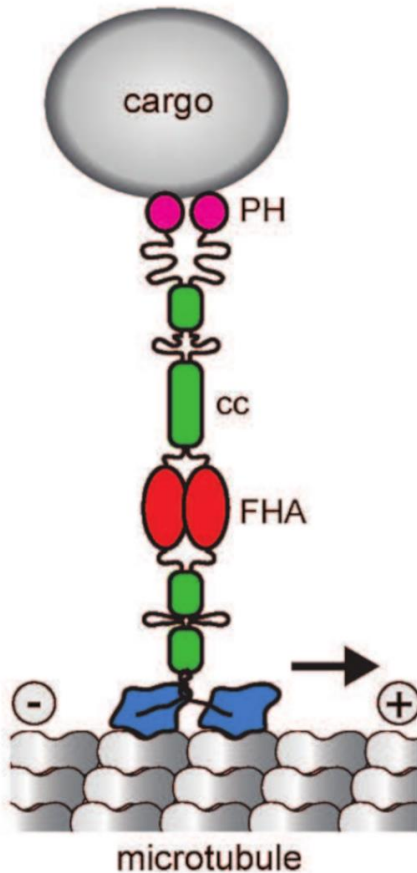


Figure 1-6: KIF1A structure and interaction with vesicles and microtubules

KIF1A is an anterograde motor protein made up of a motor domain, neck, stalk, and tail domains. The globular motor domain has an ATP and microtubule binding region, therefore, it acts as the “feet” of the motor. Adjacent to the motor domain, KIF1A has a specialized structure, the K-loop, that enhances motor processivity. The stalk region, containing FHA and CC domains, is involved in motor activation and dimerization. Finally, the kinesin tail is responsible for cargo binding via the PH domain (Siddiqui and Straube, 2017)

KIF1A processivity can be affected by multiple factors including motor activation by cargo binding and motor interactions with microtubule tracks. Because KIF1A processivity relies on binding to the microtubules, any factors that alter KIF1A’s binding affinity for microtubules, such as binding of the MAP tau, impact KIF1A movement (Hirokawa, et al., 2009). The importance of proper interactions between KIF1A, ATP, and microtubules is highlighted by the range of neuropathies and cognitive disorders associated with diverse mutations in KIF1A. For example, genetic studies have shown that individuals with mutations in the motor domain of KIF1A suffer from a range of diseases such as spastic paraparesis, cerebellar atrophy, and nerve atrophy (Lee et al., 2015).

1.4. MAPs and Axonal Transport

Microtubules play a role in several cell processes such as cell growth, division, and vesicle transport. They are highly dynamic structures that undergo constant remodeling and modifications to allow for these cellular processes to occur. Microtubules can be modified by either post-translational modifications of their subunits or by binding of proteins belonging to the MAP family. MAPs can bind to either the surface of the tubulin subunits or to the valley in between protofilaments (PFs). MAPs can associate with microtubules and regulate growth, stability, and motor protein interactions (Nogales & Zhang, 2016).

MAPs can regulate microtubule growth as well as overall shape. For example, EB proteins are structural MAPs that bind the plus-end of microtubules. They regulate microtubule dynamics by increasing the frequency in which the MTs switch from a growing phase to a shrinking phase (Nogales & Zhang, 2016). Negative-end binding MAPs, such as the CAMSAP family proteins, regulate microtubule stability, especially in long axons found in mammalian neurons (Akhmanova & Hoogenraad, 2015). Alongside EB proteins, MAP2 and tau are also structural MAPs involved in the regulation of microtubule structure in neurons. These MAP proteins are expressed in neurons and they regulate microtubule stability, rigidity, and the formation of microtubule bundles. MAP2 localizes to dendrites whereas tau localizes to axons and, in addition to the functions previously mentioned, they have unique functions depending on their specific cellular compartments. MAP2 regulates dendrite formation and elongation while tau promotes axon outgrowth by reducing the shrinkage rate of microtubules (Dehmelt and Halpain, 2005). Furthermore, tau dysregulation is heavily linked to tauopathies and Alzheimer's disease (Jeong, 2017). Specifically, hyperphosphorylated tau leads to a decrease in microtubule stability, tau aggregation, and impaired axonal transport (Venkatramani and Panda, 2019).

MAPs can also regulate microtubule interactions with motor proteins and thus allow for regulation of vesicle trafficking and localization. The differences in MAP distribution in axons and dendrites act as a local cue that further guides differential vesicle transport into either of these compartments. For example, tau distribution influences long range bidirectional transport in the axon. High concentrations of tau act as a molecular hurdle which impairs kinesin movement while favoring dynein transport

(Franker & Hoogenraad, 2013). In addition to tau, the doublecortin MAPs family, of which doublecortin proteins (DCX) and DCLK1 are members, has also been linked to regulation of kinesin transport. Knockout experiments in mice showed that deficiency in DCX and DCLK1 proteins resulted in aberrant brain structure and a deficit of SVPs in axons. This last observation indicates that they not only regulate microtubule structure, but also affect microtubule and motor protein interactions. (Deuel et al., 2006).

1.5. DCLK1

Doublecortin-like kinase 1 (DCLK1) is a regulatory MAP in the DCX family. DCX proteins are composed of two distinct domains, one at the N-terminal and one at the C-terminal. The N-terminal domain, made up of two smaller doublecortin domains (DC), binds to microtubules. Structural analysis of the interactions between members of the DCX family and MTs observed that DCX shows substrate specific binding, as it binds only to microtubules with 13 PFs. These studies also showed that DCX proteins bind to microtubules in the gaps between adjacent PFs and thereby stabilize microtubule structure by strengthening lateral connections between PFs (Moore et al., 2004). In addition to MT interaction, protein members of the DCX family interact with other proteins such as c-Jun N-terminal kinase (JNK) to regulate cell migration (Gdalyahu et al., 2004) and the motor protein KIF1A to regulate vesicle trafficking (Liu et al., 2012).

DCLK1 is present in both developing and mature mammalian neurons and interacts with KIF1A to regulate motor movement. Similar to other DCX proteins, DCLK1 is made of two distinct domains: a C-terminal and an N-terminal. The C-terminal domain includes a kinase domain, involved in regulation of cell migration, while the N-terminus has two MT binding domains; N-DC and C-DC. Structural studies of the N-terminal portion of DCLK1 showed that this protein can bind not only microtubules, but also the motor domain of KIF1A and form a ternary complex between these components. This ternary complex stabilizes KIF1A binding to microtubules. More specifically the linker portion next to the N-DC domain appears to interact with KIF1A and changes conformation depending on whether the motor protein is bound or not (Liu et al., 2012). Additionally, the microtubule-binding domain has phosphorylation sites that can be targeted by different kinases such as CDK5 and JNK. It also contains autophosphorylation sites, which indicates that DCLK1 can regulate its own microtubule binding affinity (Ramkumar et al., 2018).

Presence of DCLK1 on microtubules enhances KIF1A binding to the microtubule tracks, which suggest that differences in the amount of DCLK1 present on a microtubule could have an effect on the processivity of KIF1A movement. Research in mammalian neurons showed that absence of DCLK1 reduces the number of SVPs, a KIF1A cargo, transported out of the cell body and into axons. In these studies, quantification of vesicle movement in DCX and DCLK1 depleted neurons showed a decrease in vesicle runs and an increase in pausing, thus confirming that DCLK1 does have a direct effect in KIF1A movement (Liu et al., 2012). Furthermore, reduced DCLK1 levels in hippocampal neurons led to a decrease in DCV movement towards dendrites, further confirming that DCLK1 influences transport of KIF1A cargoes in neurons (Lipka et al., 2016). These studies suggest a potential role for differences in DCLK1 distribution to act as a local cue regulating axonal vesicle movement at synaptic sites.

1.6. Synaptic delivery

Synapses are specialized structures formed by receptors, signaling molecules, and structural proteins required for neuronal transmission (Figure 1-7; Luján et al., 2005). Synaptogenesis refers to the creation of synapses and it takes place throughout an animal's lifespan. There are different types of synapses formed in the body, and the location of the synapse on the axon varies depending on the type of synapse. Neurons in the hippocampus, and more generally throughout the cerebral cortex, can form synapses at axon terminals as well as along unmyelinated axons (Bury & Sabo, 2016). Synapses release signaling molecules during synaptic activity; synapses can undergo either spontaneous or evoked activity. In contrast to evoked activity, neurotransmitter release at spontaneous synapses occurs without the arrival of an action potential. Studies in *Drosophila* neurons have shown that synapses can undergo either spontaneous or evoked release but not both (Peled et al., 2014).

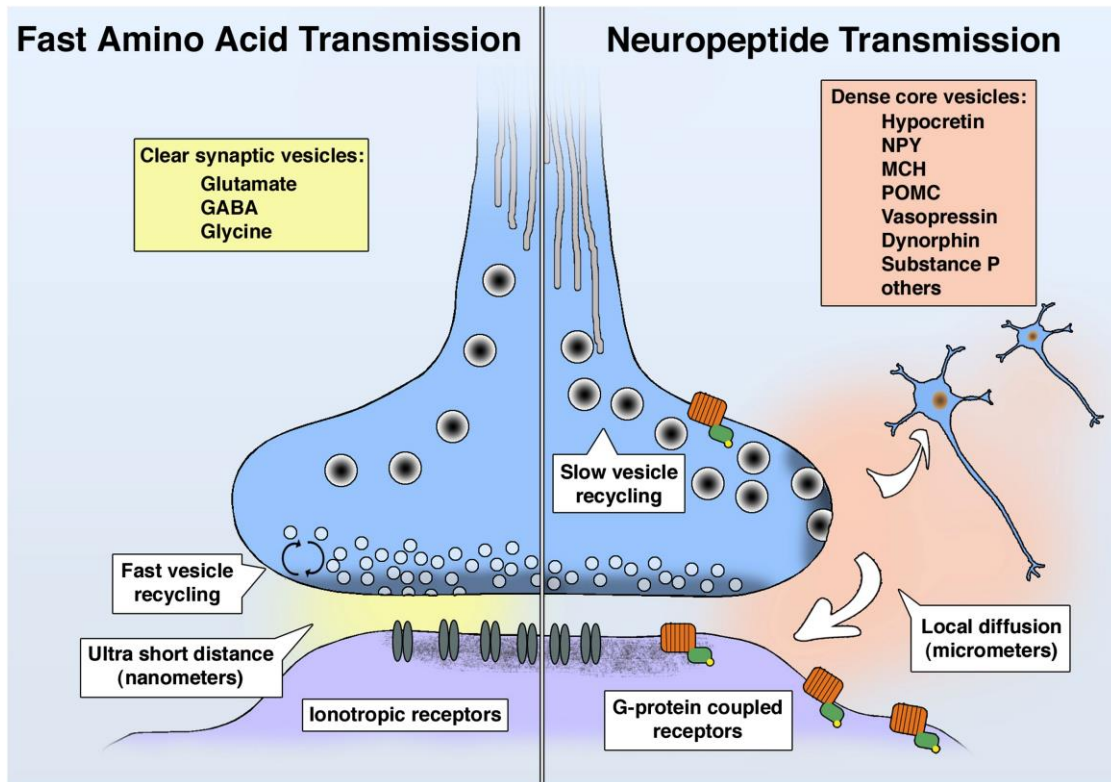


Figure 1-7: Synapse structure and composition

Synapses are specialized structures involved in intercellular communication. At pre-synaptic sites, two different types of vesicles, DCVs and synaptic vesicles, accumulate. These vesicles release signaling molecules, such as neuropeptides (right side) and neurotransmitters (left side), that bind to receptors at the post-synaptic site. (van den Pol, 2012)

Synapse formation and remodeling consists of a series of carefully regulated processes that begin when the axon and dendrite come in contact (Bury & Sabo, 2016). Contact between an axon and a dendrite causes transient binding which triggers the recruitment of trans-synaptic proteins, such as Eph receptor, neuroligin, and cadherins. Recruitment of these proteins regulates recruitment of scaffolding molecules and receptors, such as glutamate receptors, as well as actin reorganization at those sites (Hruska & Dalva, 2012). Accumulation of actin filaments at synaptic sites is essential for short-range vesicle transport into these sites. Furthermore, filamentous actin rearrangement at pre-synaptic sites also plays a role in vesicle capture (Kevenaar & Hoogenraad, 2015).

Actin filaments have two distinct ends, a fast growing, plus-end, and a slow growing one, minus-end, and are very dynamic structures, quickly going through polymerization and depolymerization cycles (Chevalier-Larsen & Holzbaur, 2006). Actin filaments act as tracks for some members of the myosin family. The myosin family

encompasses a great variety of proteins with different roles in regulation of cell migration and vesicle transport but specifically, Myosin V and VI are involved in actin-based short-distance transport of vesicles in the synaptic region. Specifically, myosin V is a plus-end motor protein responsible for anterograde transport of vesicles containing signaling molecules or receptors at the pre- and post-synaptic sites. Myosin VI is a minus-end motor involved in retrograde transport of vesicles at the pre-synaptic sites and internalization of receptors in the post-synaptic site. Cargo binding to the myosin tail domain allows it to unfold, bind the actin tracks and begin cargo transport at synapses (Hirokawa et al., 2010).

Neurotransmission at synapses depends on vesicle fusion for release of signaling molecules, therefore, both synaptic vesicles and DCVs need to accumulate at those sites. There are several steps involved in vesicle accumulation at pre-synaptic sites: vesicle delivery, cargo drop off, docking, priming and finally fusion for exocytosis (Figure 1-8; Calahorro & Izquierdo, 2018). The initial signaling cascade, regulated by neuroligin and neuexin interaction, seems to be one of the mechanisms that lead to SVP capture and docking (Bury & Sabo, 2016), however, the signaling cascade involved in DCVs pausing and capture at pre-synaptic sites is still unclear.

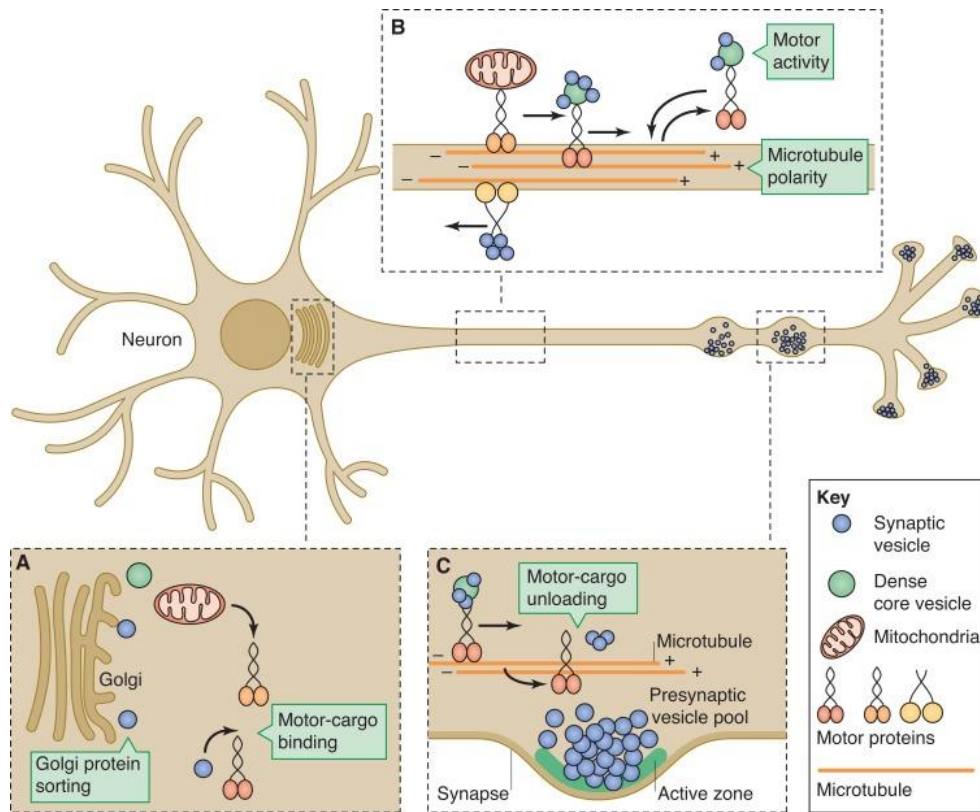


Figure 1-8: Steps for vesicle accumulation at synapses

Vesicle accumulation at synapses depends on a series of regulated steps. First, Golgi-derived vesicles, such as SVPs and DCVs, have to bind either a kinesin or dynein motor (panel A). Then, vesicles must be transported to a target location for accumulation (panel B). Once vesicles reach the target site, modifications to the motor-cargo and motor-microtubule interactions must occur to allow for vesicle pausing, cargo drop-off, and ultimately accumulation at synaptic sites (panel C) (Chia et al., 2013)

DCV accumulation at synaptic sites occurs by a combination of modifications to both motor-cargo and motor-microtubule interactions (Bharat et al., 2017; Guedes-Dias et al., 2019). Recent studies on *syt-4*, an integral membrane DCV protein, suggest that phosphorylation of *syt-4* is involved in DCV drop-off from motor proteins, which then promotes its accumulation at pre-synaptic sites. Studies in rat hippocampal neurons observed that *syt-4* phosphodeficient mutants lead to an increase in vesicle motility and reduction of vesicles present at synaptic sites, which indicates that *syt-4* phosphorylation is essential for vesicle pausing and capture. Furthermore, *syt-4* interaction with JNK, and the changes in JNK levels at capture sites after depolarization and during maturation, suggest that JNK might regulate *syt4* phosphorylation and thereby also be involved in vesicle drop-off at pre-synaptic sites (Bharat et al., 2017).

In addition to motor-cargo interactions, vesicle capture can also be regulated by modifications to the microtubule structure that affect binding of the motor proteins. A recent study focusing on the role of microtubule structure in SVP localization showed that pre-synaptic sites are enriched with GTP-tubulin ends. Accumulation of these GTP-tubulin ends destabilize KIF1A binding to the microtubules, which causes the motor protein to fall off the tracks. This pause in movement then leads to vesicle capture. Further experiments showed that a KIF1A mutant capable of binding the GTP-tubulin ends showed normal vesicle trafficking but a reduction in vesicles captured at synapses. This observation further exemplifies how weak binding of KIF1A to microtubule ends is responsible for vesicle pausing and subsequent capture (Guedes-Dias et al., 2019). Modifications to microtubules by binding of MAPs, such as DCLK1, also influence motor protein movement and pausing (Liu et al., 2012). These results suggest that modifications to the microtubules, such as MAPs binding, at pre-synaptic sites could lead to motor proteins pausing long enough to allow for vesicle capture.

1.7. Project overview

The main goal of my thesis was to understand DCV behavior as they move along the axon and to study the mechanism that regulates DCV accumulation at synapses. To do so, my research focused on observing DCV behavior at two different stages of transport. DCV movement was tracked while the vesicles traveled along the axon and then as they approached pre-synaptic sites. To better understand DCV accumulation in synapses, I was also interested in understanding the regulation of KIF1A pausing at capture sites. The 3 specific goals of my thesis were:

1. Understand DCV trafficking patterns as they move along the axon.

Studies in *Drosophila* neurons revealed that DCV follow a conveyor belt pattern as they travel along the axon. Furthermore, recent studies in mammalian neurons proved that DCV also move bidirectionally while they travel down the axon (Bharat et al., 2017a). My thesis focused in quantifying different parameters of DCV trafficking behavior as they move bidirectionally in the axon.

2. Observe DCV behavior as they approach synaptic sites.

DCV accumulation at synaptic sites is essential for proper synapse function, therefore, tracking DCV movement as they approach these sites could be key in improving our understanding of synapse formation. Because DCVs trafficking behavior near synaptic sites had not been studied in mammalian neurons before, my second aim was to determine whether DCVs capture depends on the direction of vesicle movement.

3. Assess the effect of DCLK1 in KIF1A pausing for DCV capture at synaptic sites.

Accumulation of DCVs at synapses depends not only on correct vesicle trafficking along the axon but also on the regulation of motor pausing at synapses for vesicle capture. Because a clear mechanism by which DCV pausing occurs at synapses has not been described yet, my research aimed to determine whether the absence of DCLK1, A MAP protein and KIF1A movement modulator, might cause KIF1A pausing at synapses and thus allow for DCV capture.

Chapter 2.

Materials and Methods

2.1. Hippocampal cell culture and gene transfection

Primary hippocampal neurons were prepared from E18 rat embryos exactly as described by Kaech and Banker (Kaech and Banker, 2006). Neurons were plated on glass coverslips pre-treated with poly-L-lysine (Sigma-Aldrich) and allowed to develop in 6 cm tissue culture dishes containing a layer of astrocytes in SM1/Neurobasal media (StemCell/Corning).

At 5 and 10 days in vitro (DIV), neurons were transfected with plasmids expressing a dense core vesicle marker, BDNF-RFP (gift of G. Banker, OHSU), and a synaptic vesicle marker, Synaptophysin-GFP (Syn-GFP; gift of B. Scalettar), using EndoFectin (GeneCopoeia), according to manufacturer's instructions. For each transfection, 2 μg of DNA for each plasmid was mixed with 10 μl of EndoFectin in 500 μl of MEM. Prior to transfection, 0.5 μM kynurenic acid (Sigma-Aldrich) were added to each a dish to decrease excitotoxic damage. Cells were incubated with the transfection mixture and allowed to express the construct for 24 to 36 hours before live imaging. All experiments with animals were approved by and followed the guidelines set out by Simon Fraser University Animal Care Committee, Protocol 943-B05.

2.2. Live Imaging

To analyze vesicle trafficking in neurons, hippocampal neurons were imaged using a wide-field fluorescent microscope (DMI, 6000B Leica) equipped with a CCD camera (Hamamatsu Orca-ER-1394). Following transfection, cells were mounted in a heated chamber containing imaging media (Hank's balanced saline solution, 20% glucose, HEPES) and imaged with a 63X/1.40 lens using immersion oil (Cargill; type DF). After morphological identification of the cell body and the axons, videos of vesicle movement in distal segments of the axon were obtained using MetaMorph (Molecular Devices, Sunnyvale, CA). Videos were made by acquiring 4 frames per second for up to

4 min. The obtained videos were then used to generate kymographs in MetaMorph for further analysis.

2.3. Vesicle movement analysis

The videos obtained were then used to generate kymographs, time versus position graphs, using MetaMorph (Kwinter et al., 2009). Vesicle movement parameters, such as flux, speed, and run lengths, were then quantified by tracking vesicle movement in the kymographs. Anterograde and retrograde movement were quantified by tracing positive and negative slopes, respectively; stationary vesicles were represented by straight flat lines. Only runs over to 2 μm long were traced to avoid tracing movement that could be due to diffusion rather than motor protein movement. Places with accumulation of stationary Syn-GFP and BDNF-RFP were marked as synaptic sites. Vesicle capture at synaptic sites and reversal events were quantified manually. After the kymographs were traced, they were analyzed using a custom software as described in Kwinter et al. (Kwinter et al., 2009). All data obtained were calculated with the calibration that at a 630X magnification, 1 pixel= 0.160508 μm ; the generated values were collected and further analyzed in Excel.

2.4. Immunocytochemistry

For antibody staining, neurons were fixed with 4% paraformaldehyde, permeabilized using a 0.25% solution of Triton-PBS and then blocked with 0.5% fish skin-gelatin. All primary antibodies were diluted using the 0.5% fish-skin gelatin solution (Kwinter et al., 2009). To observe DCLK1 cells were stained with rabbit-anti-DCLK1 antibody (1:500, made and gifted by J. Liu; 1:500), chicken-anti-Homer (1:1000, Synaptic systems), mouse-anti-chromogranin A (1:50, Synaptic systems), and mouse-anti-synapsin (1:500, Synaptic Systems). All cells were incubated with the primary antibodies at 37° for 3 hours or at 4°C overnight. After the incubation period, excess of primary antibody was rinsed using PBS and then the neurons were incubated with the corresponding secondary antibodies: anti-chicken-488 (1:500, Synaptic systems), anti-rabbit-Cy3 (1:500, ThermoFisher) or anti-rabbit-Cy5 (1:500, Jackson ImmunoResearch Laboratories). Neurons were then mounted using either elvanol or ProLong glass antifade mountant (Invitrogen) and imaged using wide-field fluorescent microscopy or

super-resolution microscopy (Zeiss, LSM880). The resolution limit for the super-resolution microscope is 140 nm laterally and 400 nm axially.

2.5. Image analysis

Images collected from immunostained neurons were analyzed using ImageJ software (Rueden et al., 2017). Initially, to assess co-localization between DCLK1 and BDNF-RFP and DCLK1 and synaptic sites a linescan analysis was performed. In this analysis, axons, or regions of interest, were manually traced and peaks of fluorescence intensity were measured along those lines. Each peak in fluorescence represented puncta from one of the markers. Sites of overlap of BDNF-RFP and Syn-GFP peaks were marked as synapses. Co-localization of peaks of fluorescence was then qualitatively evaluated to determine whether DCLK1 is present at potential pre-synaptic sites.

After linescan analysis, to assess whether DCLK1 is present or absent at synaptic sites, co-localization analysis was done using immunostained neurons. Quantification of co-localization was done by measuring the distance between puncta of the three markers using a similar approach used by Poburko et. al. (Mojard Kalkhoran et al., 2019). In this approach, puncta for each marker were identified using Recursive ImageJ Particle Analyzer segmentation (RIPA). Once the regions of interest (ROIs) for the puncta were generated, the nearest neighbour (NN) between the ROIs of one marker, acting as a reference channel, and the ROIs of the other two were quantified. This analysis was performed using the MINER macro built and modified by Dr. Damon Poburko (Kalkhoran et al., 2019). By measuring the percentage of DCLK1 present at synaptic sites, marked by co-localized synapsin and Homer or co-localized chromogranin A and synapsin, I quantified whether DCLK1 puncta is absent from synaptic sites. Interaction of DCLK1 and DCVs was also quantified using this approach.

2.6. Statistical analysis

Data obtained from kymograph analysis was compiled and further analyzed using Excel. Parameters obtained from vesicle movement analysis are presented box and whiskers graphs showing the distribution of the data and the average values. Dots outside the whiskers represent outlier data points greater than the values in the first or

third quartile by 1.5 times the interquartile range. In the live imaging experiment, 21 cells from at least 5 independent cultures were analyzed. Statistical analysis of the data from the immunocytochemistry experiment and MINER analysis was processed by using JMP (JMP®, Version 14. SAS Institute Inc., Cary, NC, 1989-2019) and Excel.

Chapter 3.

Results

3.1. DCV movement down the axon

DCVs transport and release signaling molecules at synapses, therefore, accumulation of DCVs at synaptic sites is necessary for correct synapse function. Studies of DCV movement in *Drosophila* showed that these vesicles move following a pattern resembling a “conveyor belt” when they move along the axon (Wong et al., 2012). Although *Drosophila* neurons are a good model for these studies, they are vastly different to mammalian neurons in size and complexity. For example, mammalian neurons can have highly branched axons and be up to 1 meter in length (Franker and Hoogenraad, 2013). Because of the morphological differences, the first aim of my thesis was to study axonal DCV movement in hippocampal neurons to determine whether DCVs show the same trafficking behavior observed in *Drosophila*.

To achieve my first goal, I transfected rat hippocampal neurons with a DCV marker (BDNF-RFP) to track vesicle movement. Neurons were also transfected with an SVP marker (Synaptophysin-GFP) to study DCV movement near capture sites in a later experiment (section 3.2). 24 hours after transfection, I used live imaging using fluorescent microscopy to track axonal DCV movement (Figure 3-1A). Subsequent kymograph analysis of DCV trafficking showed anterograde vesicle movement, marked by positive slope lines, as well as retrograde movement, marked by negative slope lines. Stationary vesicles, marked by flat lines, are also observed. In addition to anterograde and retrograde movement, the kymographs also showed switches in vesicle direction (Figure 3-1B).

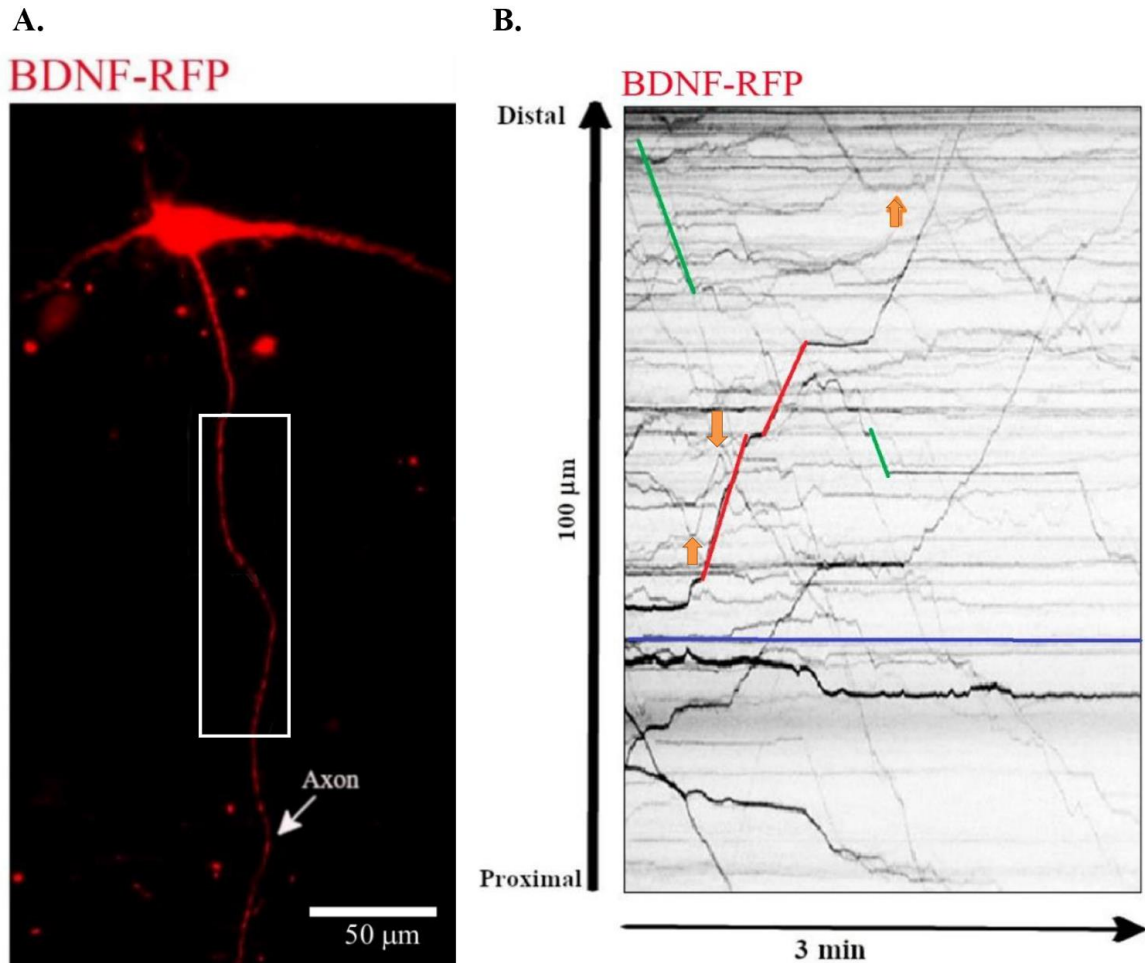


Figure 3-1: DCVs move bidirectionally as they travel down the axons and can undergo reversal events.

A) Puncta observed in neurons transfected with a DCV marker, BDNF-RFP. Movement of DCVs in the mid and distal axon was tracked using live-fluorescence microscopy and used to generate kymographs. The area highlighted the portion of the axon used to generate the kymograph in the left panel. B) Kymograph of DCV movement in a 5 DIV transfected neurons. Examples of anterograde movement (red), retrograde movement (green) are highlighted. Stationary vesicles are marked by flat lines (blue line). Examples of reversal events are marked by orange arrows.

Quantification of DCV movement showed that the same proportion of anterograde and retrograde events occurred in the axon. Out of 2128 movement events observed in 21 cells from five independent cultures, 1036 were anterograde events and 1092 were retrograde events (Figure 3-2A). Although infrequent, a total of 178 reversal events were observed. Furthermore, I observed that DCVs moved at similar speeds when traveling in either direction; $1.9 \mu\text{m/s} \pm 0.39$ anterogradely and $1.8 \mu\text{m/s} \pm 0.41$ retrogradely (Figure 3-2D). Vesicles also exhibited similar run lengths regardless of their traveling direction; anterograde vesicles showed $5 \mu\text{m} \pm 1.94$ run lengths and

retrogradely showed $4.9 \mu\text{m} \pm 2.46$ run lengths (Figure 3-2C). These results show that both kinesin and dynein motor proteins have similar processivity and that there is no directional bias as vesicles travel along the axon.

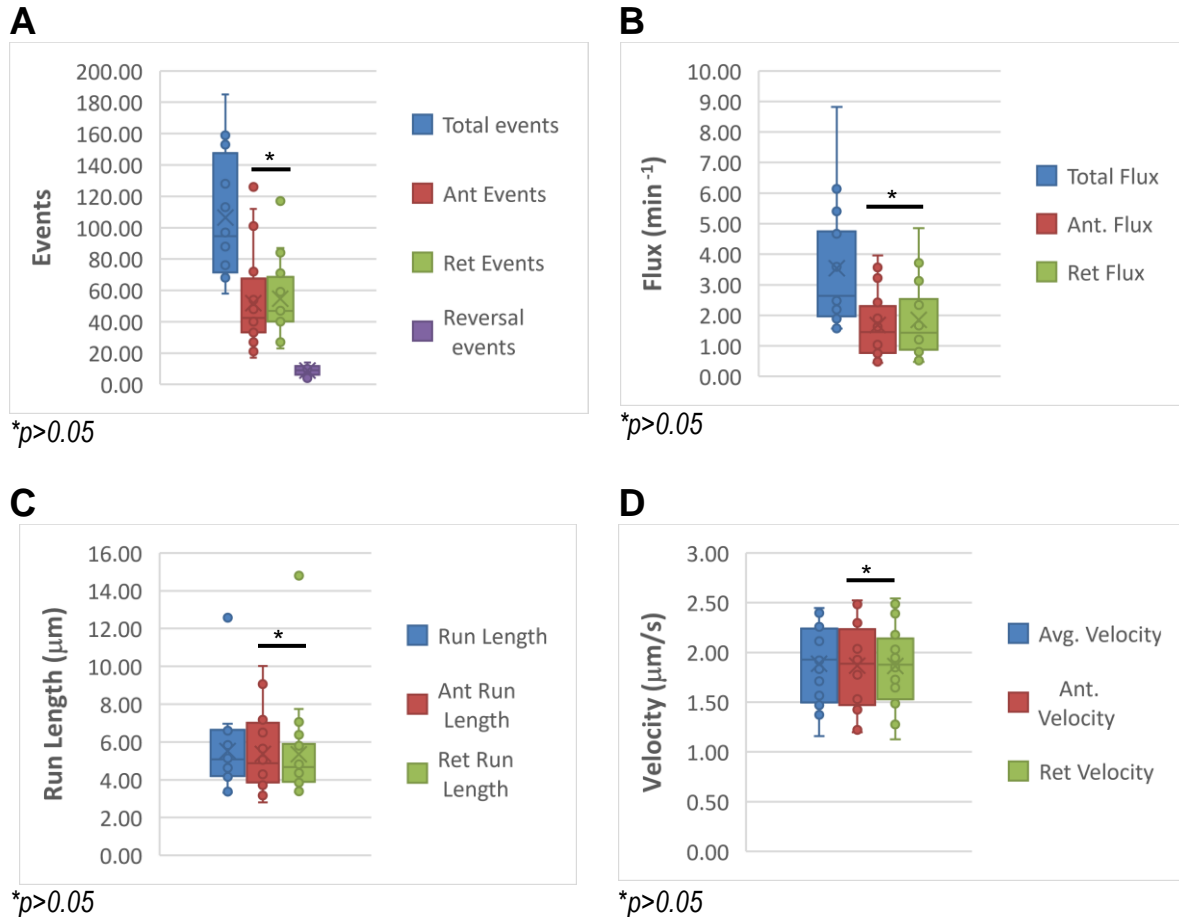


Figure 3-2: DCVs exhibit bidirectional trafficking behaviour.

Number of events, flux, velocity and run length for axonal DCV movement was measured using kymograph analysis. Data for these parameters is depicted in bar graphs where the median is represented by an inner line and the mean by an X. First and third quartiles are represented by bottom and top of the box. Data range is marked by the whiskers and dots outside the bars represent outliers. A) Quantification of total number of movement events and proportion of anterograde, retrograde and reversal events. There is no difference between the number of anterograde and retrograde events. A small proportion of reversal events at different points in the axon is observed. B) Measurement of anterograde and retrograde flux. Flux values are similar for anterograde and retrograde movement. C) Average anterograde and retrograde run lengths. Vesicles showed similar run lengths as they travel down the axon. D) Average velocity for anterograde and retrograde movements. Vesicles traveled at similar velocities along the axon. N= 21 cells and 2128 events from 5 different cultures.

3.2. DCV behavior near synaptic sites

Observations in *Drosophila* neurons showed that vesicles traveling both anterogradely and retrogradely can be captured at synaptic sites (Wong et al., 2012). To determine whether this behavior also occurs in mammalian neurons, the second aim of my project focused on tracking DCVs as they approach synaptic sites.

To study DCV capture in mammalian neurons, I used doubly transfected neurons (as described in the previous section) to track movement of DCVs, containing BDNF-RFP, and SVPs, containing Syn-GFP (Figure 3-3). Using both live-imaging videos and kymograph analysis, I defined synaptic sites as places where there was accumulation of stationary Syn-GFP and BDNF-RFP (Figure 3-4). The studies performed in *Drosophila* neurons defined capture sites as places where vesicles remained stationary for over 5 minutes (Wong et al., 2012). In contrast, studies in mammalian neurons defined capture sites as places where vesicles remained stationary for over 2 minutes (Bharat et al., 2017a). To distinguish pausing events from capture, only DCVs that became stationary at synaptic sites for at least three minutes were counted as captured. Using kymograph analysis, I quantified the number of capture events as well as the direction that the vesicles were traveling before capture.

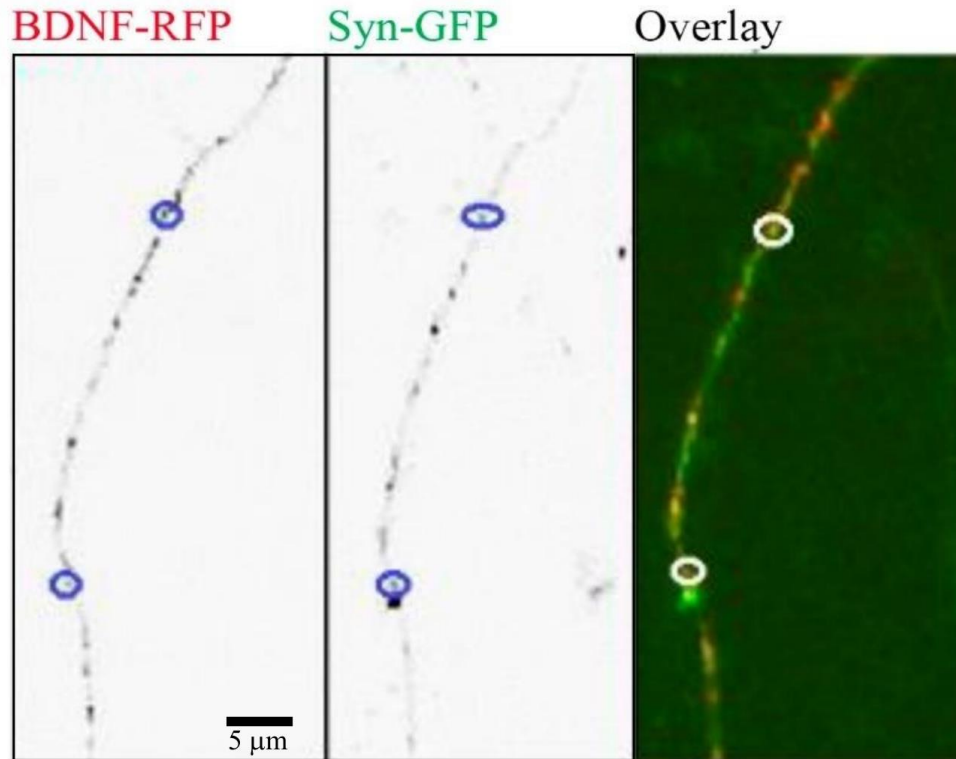


Figure 3-3: Capture sites in axons.

Region of an axon from a 5DIV neuron transfected with BDNF-RFP and Syn-GFP. Regions of overlap of stationary SVPs (green) and DCVs (red) are considered potential pre-synaptic sites. Examples of accumulation of Syn-GFP and BDNF-RFP are highlighted by circles. Places of accumulation of SVPs and DCVs were further confirmed as pre-synaptic sites using kymographs such as the one seen in figure 3-4.

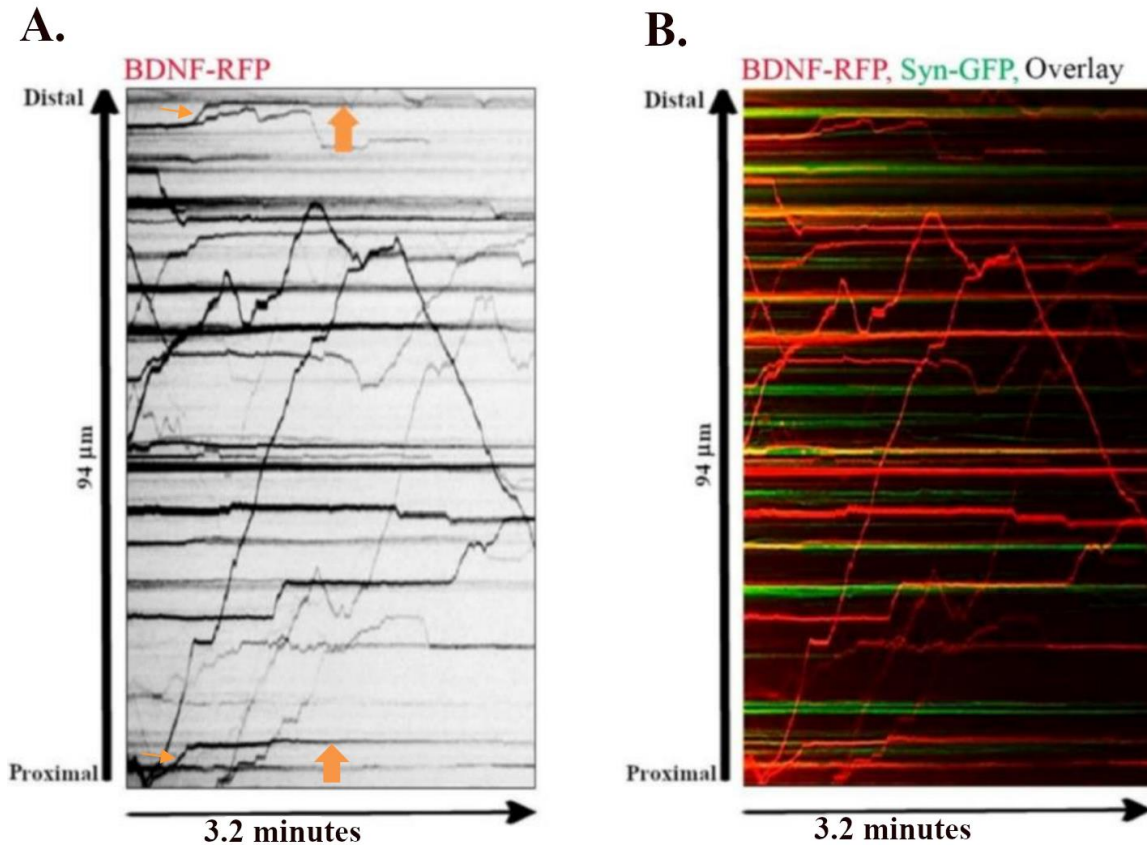


Figure 3-4: DCVs can be captured at pre-synaptic sites regardless of their direction of movement.

Segment of kymographs following DCV and SVP movement in 5 DIV transfected neurons. Neurons were transfected with BDNF-RFP and Syn-GFP and imaged 24 hours post-transfection. A) Kymograph of DCV movement. Vesicle movement was tracked for over 3 minutes B) Overlay of a DCV kymograph (red) and an SVP kymograph (green). Events where DCV vesicles pause for over 3 minutes at sites with accumulation of SVPs, marked by flat green lines, were counted as capture events. Examples of vesicles captured are marked by orange arrows in panel A. Thin arrows mark portions of vesicle movement prior to capture. Thick arrows mark captured vesicles. The image displayed on figure 3-4 was part of the same data set used for figure 3-2.

Data obtained from 21 neurons from five different cultures showed that capture events were rare. Out of the total number of movement events observed (2128), a small number of vesicles are captured (40). This finding indicates that only 1.9% of all the trafficking events observed lead to DCV capture. Comparison of the direction of capture events showed that DCVs can be captured while traveling in either direction. From a total of 40 capture events observed, 24 occurred while the vesicle was traveling anterogradely and 16 while the vesicle traveled retrogradely (Table 3-1). Anterograde events occur 1.5 times more often than retrograde events, which suggested an anterograde bias for DCV capture in axons. However, after chi square analysis, I observed that there is not a statistically significant difference in the number of

anterograde versus retrograde capture events as the chi square value, 1.6, was less than the critical value, 3.84, for this set of data.

Table 3-1: DCV capture can occur regardless of the direction of vesicle movement in axons

	Total	Capture	Anterograde capture	Retrograde Capture
Number of events	2058	40	24*	16*
average events/cell	195.7	2.2	1.3	0.9

Table summarizing total number of capture events. Capture events were grouped depending on the direction in which the DCV was traveling prior to capture. Capture events occurred from both anterograde and retrograde movement. Furthermore, the number of anterograde versus retrograde events indicate an anterograde bias in vesicle capture. Capture events were quantified from 21 cells from 5 different cultures.

* χ^2 value = 1.6, therefore the $\chi^2 <$ critical value (critical value = 3.841)

3.3. Presence of DCLK1 at synaptic sites

Vesicle pausing is an essential step that leads to vesicle capture and accumulation at synapses, therefore, my last aim focused on understanding the regulation of KIF1A pausing near synaptic sites. To study this, I focused on determining whether absence DCLK1 from synaptic sites facilitated KIF1A pausing at synapses. Because the role of DCLK1 in DCV transport had only been studied in dendrites, I first confirmed whether DCLK1 is present in axons. To assess the presence of DCLK1 in both axons and dendrites, 10 DIV hippocampal neurons were stained with an anti-DCLK1 antibody and either a dendritic marker, anti-MAP2, or an axonal marker, anti-Paired Helical Filaments-tau (PHF). Images of immunostained neurons showed that DCLK1 was present in processes positive for MAP2, thereby confirming DCLK1 in dendrites (Figure 3-5A). Moreover, DCLK1 was also observed in processes stained with PHF, thus confirming that DCLK1 is present in axons (Figure 3-5B).

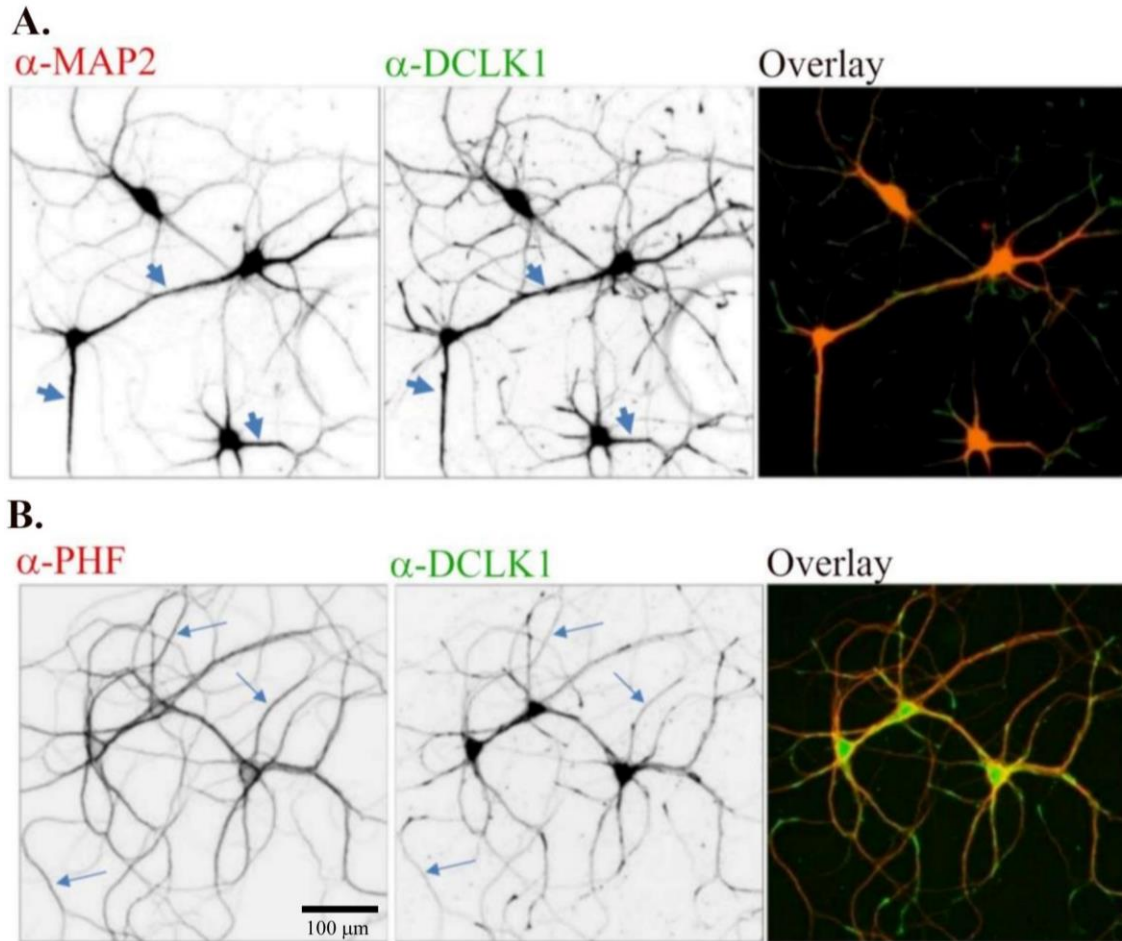


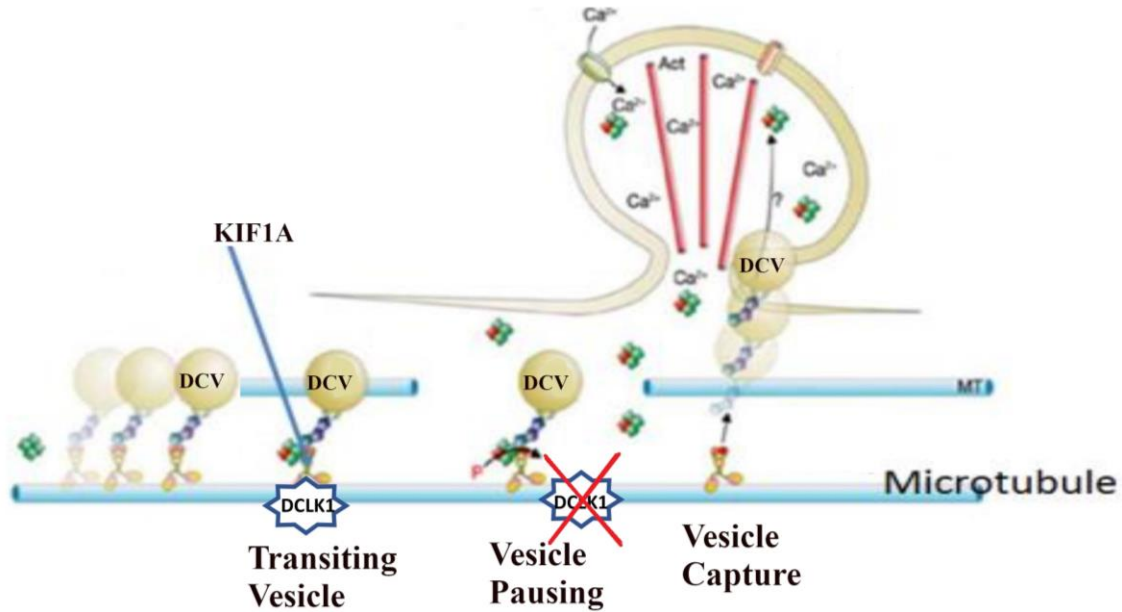
Figure 3-5: DCLK1 is present in both axons and dendrites.

A) Neurons stained with a dendritic marker, anti-MAP2 (red) and anti-DCLK1 (green). Regions of overlap of anti-MAP2 and anti-DCLK1 confirm presence of DCLK1 in dendrites. Examples of dendrites with DCLK1 and MAP2 are marked by thick arrows B) Neuron stained with an axonal marker, anti-PHF (red) and anti-DCLK1 (green). Regions of anti-PHF and anti-DCLK1 overlap confirm presence of DCLK1 in axons. Examples of PHF and DCLK1 overlap in axons are marked by thin arrows.

Next, to determine whether DCLK1 regulates DCV pausing at synaptic sites, I assessed the co-localization of DCLK1 with axonal DCVs and the co-localization of DCLK1 with synaptic sites. Initially, using transfected neurons stained with anti-DCLK1, I evaluated whether there was co-localization between BDNF-RFP (DCV marker) and DCLK1 and whether DCLK1 was present at synaptic sites, marked by accumulation of BDNF-RFP and Syn-GFP. Then, in the next two experiments I quantified the percentage of co-localization between DCLK1 and chromogranin A (DCV marker) and DCLK1 and synapses. In these co-localization experiments, synapses were marked by either co-localized synapsin and Homer or co-localized synapsin and chromogranin A. A summary

of the combinations of markers studied for co-localization and the interpretation of the possible outcomes is shown in figure 3-6. The presence of DCLK1 at synaptic sites was measured to determine whether the absence of DCLK1 might weaken KIF1A binding to microtubules and allow KIF1A to dissociate from microtubules, thereby regulating KIF1A pausing and vesicle accumulation at synapses.

Synapse



Interpretation:	Synapse	Transiting vesicle	Synapse	Synapse	Transiting vesicle
Marker	BDNF-RFP ●	BDNF-RFP ●	Anti-synapsin ●	Anti-synapsin ●	Anti-synapsin
Marker	Syn-GFP ●	Syn-GFP	Anti-Homer ●	Anti-chromogranin A ●	Anti-chromogranin A ●
Marker	Anti-DCLK1	Anti-DCLK1 ●	Anti-DCLK1	Anti-DCLK1	Anti-DCLK1 ●

Figure 3-6: Visual summary of the potential co-localization outcomes between the different markers and their interpretation.

Sites of co-localized vesicles, i.e., BDNF-RFP and Syn-GFP and synapsin and chromogranin A, were marked as synapses. Similarly, sites of co-localized synapsin and homer were also considered to be synapses. Absence of DCLK1 at these sites is expected. Furthermore, co-localization of a DCV marker with DCLK1 would indicate the existence of a transiting vesicle. (Adapted from Guillaud et al., 2008)

Initially, DCLK1 co-localization with DCVs and synaptic markers was studied using linescan analysis (ImageJ) in neurons transfected with BDNF-RFP and Syn-GFP and then stained with anti-DCLK1 (Figure 3-7A). Linescan analysis measured fluorescence along the axon; peaks of fluorescence are regions of either BDNF-RFP, Syn-GFP or DCLK1 puncta. Sites of overlapping peaks of BDNF-RFP and Syn-GFP, indicating accumulation of SVPs and DCVs, were considered synapses. By manual quantification of the overlapping peaks, I observed that approximately 15% of Syn-GFP peaks overlapped with DCLK1 peaks, whereas peaks of BDNF-RFP overlapped with DCLK1 peaks approximately 10% of the time. Finally, 8% of DCLK1 peaks were present at places marked as synaptic sites (Figure 3-7B).

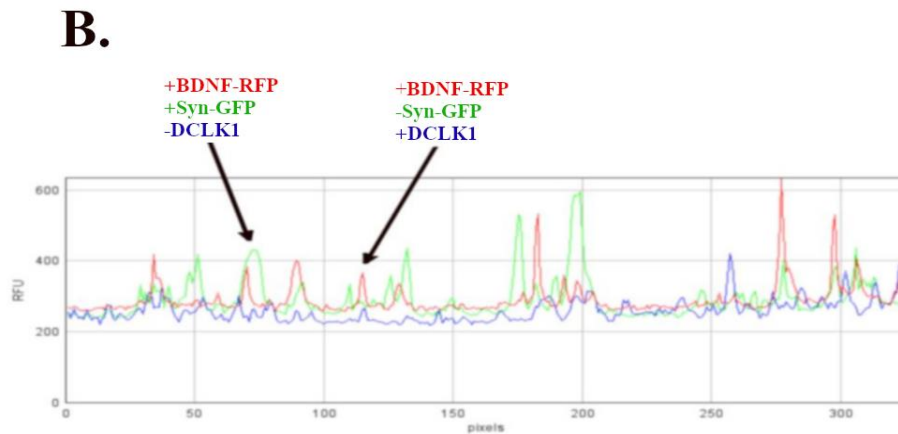
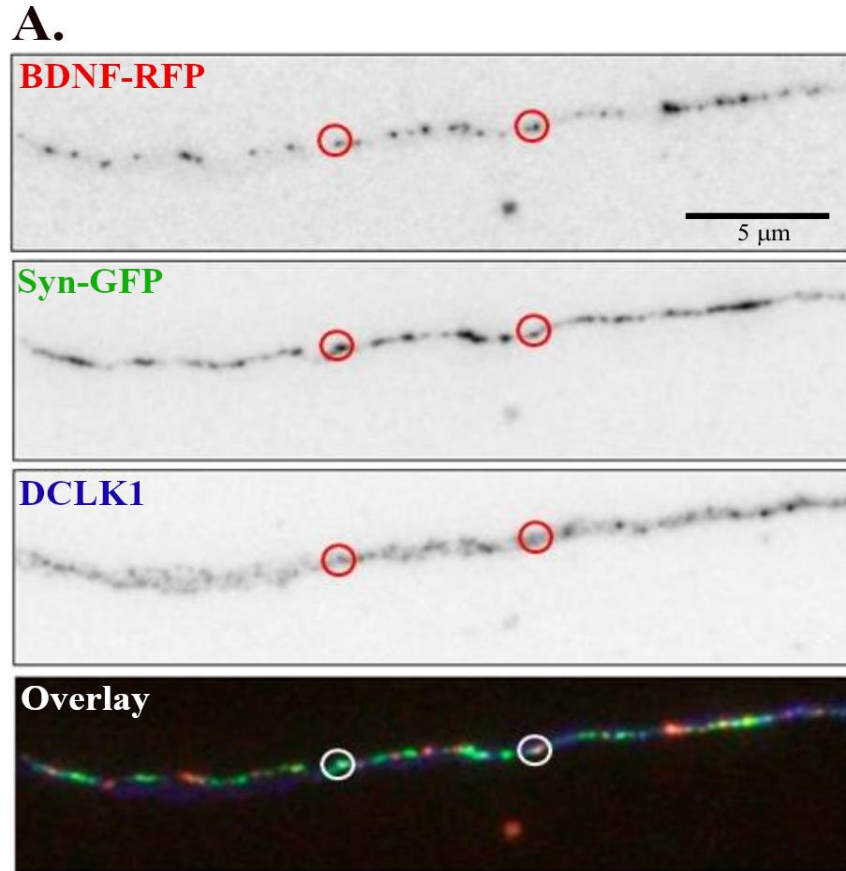


Figure 3-7: DCLK1 is absent from places where DCVs and SVPs co-localize.
 A) Regions of an axon from a 10 DIV neuron. Neurons were transfected with BDNF-RFP (DCV marker, red) and Syn-GFP (SVP marker, green) and then stained with an anti-DCLK1 antibody (blue). Places with co-localized BDNF-RFP and Syn-GFP are considered synapses. Examples of synapses where DCVs and SVPS co-localize but no DCLK1 is observed are marked by white circles. B) Linescan analysis of the axon observed in figure A. Each fluorescence peak represents puncta from one of the markers. Places where BDNF-RFP and Syn-GFP peaks accumulate are considered pre-synaptic sites. Co-localization of DCLK1 was assessed by observing whether DCLK1 peaks are present at pre-synaptic sites. Initial linescan analysis showed that 8% of DCLK1 peaks were present at places of DCV and SVP accumulation. Furthermore, this analysis showed that 10% of BDNF-RFP peaks overlapped DCLK1 peaks when BDNF-RFP is not at a synaptic site.

The initial results obtained using wide-field fluorescence microscopy and linescan analysis showed that a small percentage (8%) of DCLK1 was present at places of vesicle accumulation. Although useful for an initial assessment of DCLK1 levels at pre-synaptic sites, linescan analysis had some disadvantages, such as limited reduction of background signal and limitations for the quantification of co-localized peaks. Therefore, I performed MINER analysis on immunostained neurons next. The MINER analysis macro uses regions of interest (ROIs) of a reference channel and measures whether they have near neighbour ROIs from other channels at a set distance. MINER analysis allowed for accurate quantification of co-localization between the three different markers because co-localization was measured only between selected ROIs, thereby significantly reducing background signal. Furthermore, by using MINER analysis, I was able to quantify co-localization between three channels simultaneously and able to distinguish between co-localized and adjacent vesicles.

To quantify presence of DCLK1 at synaptic sites, neurons were immunostained with two different sets of markers. One set of neurons was stained with anti-DCLK1 along with a pre-synaptic vesicle marker (anti-synapsin) and a post-synaptic marker (anti-Homer) to mark synaptic sites. The other set was stained with anti-DCLK1 along with anti-chromogranin A and anti-synapsin to mark synaptic sites. Both sets of immunostained neurons were imaged using super-resolution microscopy and then analyzed using the MINER macro in ImageJ (Kalkhoran et al., 2019). Vesicles were considered to be co-localized when the ROI centers were less than 300 nm away from each other.

First, super-resolution images of neurons stained with synapsin, Homer, and DCLK1 were used to measure co-localization of DCLK1 at synaptic sites. To do so, the presence of Homer and DCLK1 around synapsin ROIs was scored. Places of co-localization between synapsin and Homer were counted as synaptic sites. MINER analysis showed that 1.65% of synapsin vesicles had a Homer partner and were considered synaptic sites (Table 3-2; Figure 3-8). Further co-localization analysis indicated that DCLK1 was present in 39% of the sites where synapsin co-localized with Homer.

Table 3-2: DCLK1 co-localizes with one third of synaptic sites.

Marker	Marker	% of co-localization	% DCLK1 present at synapses	Average distance between markers
Synapsin	Homer	1.70%	----	159 nm ± 90.3
Synapsin	DCLK1	18.20%	----	151 nm ± 111.8
Synaptic site (synapsin +Homer)	DCLK1	----	38.90%	

Table summarizing co-localization values for synapsin and Homer, synapsin and DCLK1, and DCLK1 at synaptic sites. Synapsin was used as the reference channel for MINER analysis. Synaptic sites were defined as places where synapsin and Homer co-localized, the percentage of DCLK1 present at these sites was measured. Co-localization analysis showed that DCLK1 was present at 39% of synaptic sites.

Data was obtained from analyzing 3270 synapsin puncta from 18 different cells from two different cultures.

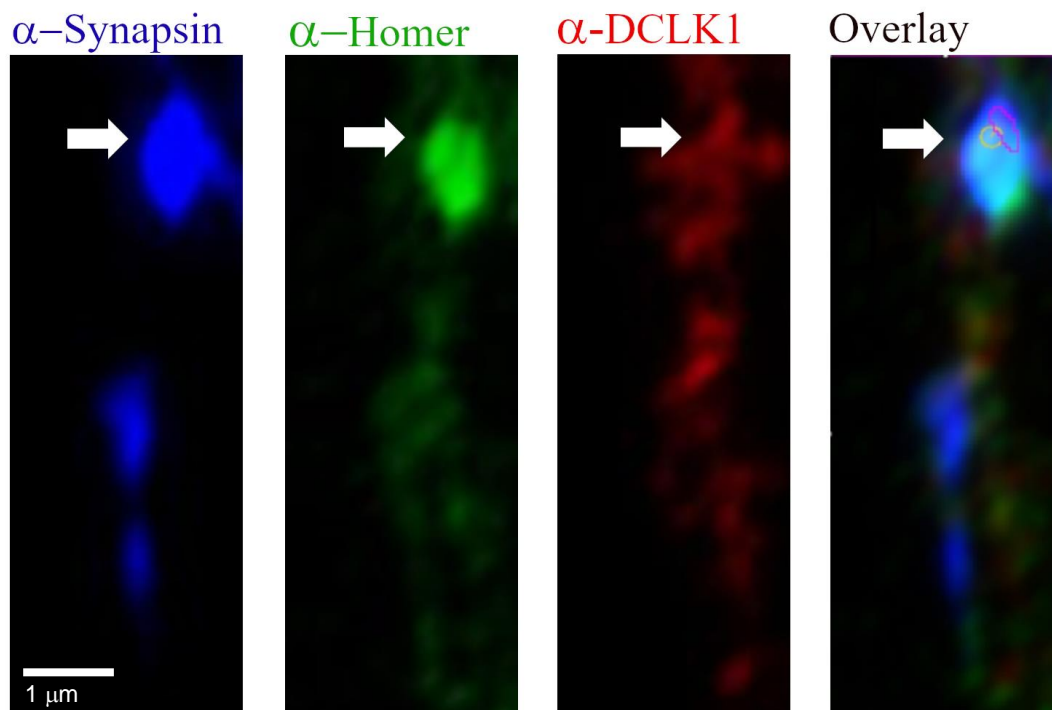


Figure 3-8: DCLK1 is absent from 61% of places with accumulated synapsin and Homer.

Region of a neuron stained with anti-synapsin (blue), anti-Homer (green), and anti-DCLK1 (red). Synapsin was used as the reference channel for MINER analysis. Places of co-localized synapsin and Homer were marked as synapses. An example of a synapse is highlighted by an arrow: DCLK1 is absent from the marked synapse. Quantification of DCLK1 at synapses showed that DCLK1 is absent from 61.1% of synaptic sites.

The results of co-localization analysis from the previous experiment showed that DCLK1 is absent from two thirds of synaptic sites. In the next experiment, I analyzed neurons stained with anti-synapsin, anti-chromogranin A, and anti-DCLK1 to quantify co-localization between DCVs and DCLK1, and to test whether a similar value of DCLK1 co-localization can be obtained using different markers for synaptic sites. The percentage of co-localization between chromogranin A and DCLK1, and DCLK1 and synapses was quantified using MINER analysis.

In order to quantify absence of DCLK1 at synaptic sites, I used co-localized chromogranin A and synapsin puncta to mark synaptic sites; these sites were then used to measure the percentage of DCLK1 present at synapses. Quantification of the percentage of synapsin and chromogranin A co-localized showed that 17.75% of the chromogranin A vesicles co-localized with a synapsin partner (Table 3-3). Quantification of DCLK1 at these synaptic sites indicated that DCLK1 was present in 34.20% of all synaptic sites with vesicle accumulation (Figure 3-9; table 3-3). The percentage of synapses without DCLK1 is similar to the value observed in the previous experiment (39%; Table 3-2) and therefore, based on both co-localization analyses, I observed that DCLK1 is, on average, absent from over 60% of synaptic sites.

Table 3-3: DCLK1 is present in one third of synaptic sites.

Marker	Marker	% of co-localization	% DCLK1 present at synapses	Average distance between markers
Chromogranin A	Synapsin	17.75%	-----	184 nm ± 106
Chromogranin A	DCLK1	21.64%	-----	185 nm ± 90
Synaptic site (Chromogranin A + Synapsin)	DCLK1	-----	34.20%	-----

Table summarizing percentage of co-localization between chromogranin A and synapsin, chromogranin A and DCLK1, and synaptic sites and DCLK1. Chromogranin A was used as the reference channel for MINER analysis. Co-localization analysis showed that axonal DCVs rarely interact with DCLK1 (21% co-localization). Places where synapsin and chromogranin A co-localized were scored as synaptic sites. Similar to the results found in the previous experiment, DCLK1 is present at one third of synaptic sites (34% co-localization).

Data was obtained from analyzing 3887 synapsin puncta from 20 different cells from two different cultures.

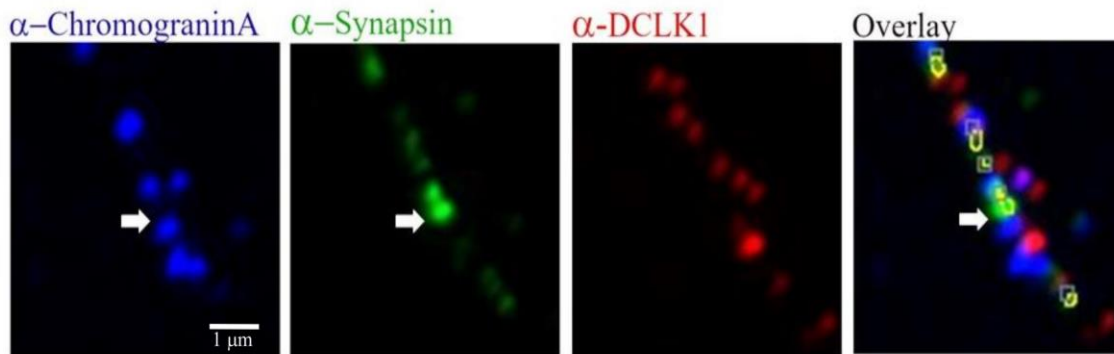


Figure 3-9: DCLK1 is absent from 66% of synaptic sites

Region of an axon from a neuron stained with anti-chromogranin A (blue), anti-synapsin (green) and anti-DCLK1 (red). Places of co-localized chromogranin A and synapsin were marked as synapses. An example of a synapse is highlighted by a white arrow; DCLK1 is absent from the marked synapse. Quantification of DCLK1 at synapses showed that DCLK1 is absent from 67.8% of synaptic sites.

To measure DCLK1 interaction with DCVs, co-localization analysis between chromogranin A and DCLK1, and synapsin and DCLK1 was performed. Co-localization of synapsin and DCLK1 was measured as a negative control. Because synapsin is not a KIF1A cargo, low co-localization between synapsin and DCLK1 was expected. As expected, 18% of synapsin was co-localized with DCLK1. Quantification of the percentage of DCVs co-localized with DCLK1 showed that 21% of axonal DCVs co-localized with DCLK1 (Table 3-3; Figure 3-10). The percentage of synapsin puncta co-

localized with DCLK1 (18%) was similar to the co-localization percentage of DCLK1 and DCVs (21%), which indicates that DCLK1 might not regulate DCV movement in axons.

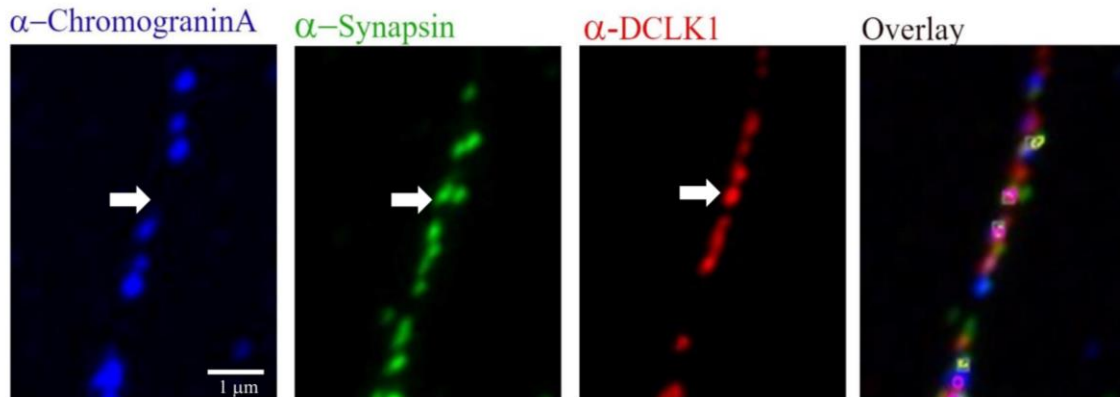


Figure 3-10: DCLK1 co-localizes with 21% of axonal DCVs.

Zoomed in regions of an axon from a neuron stained with anti-chromogranin A (blue), anti-synapsin (green) and anti-DCLK1 (red). Chromogranin A puncta were used as a reference channel for MINER analysis. Co-localization analysis between DCLK1 and chromogranin A showed that 21% of chromogranin A co-localize with DCLK1 puncta. An example of synapsin and DCLK1 co-localization with DCLK1 and absence of chromogranin A is marked by a white arrow.

Although DCLK1 did not co-localize with 79% of axonal DCV puncta, both MINER analyses showed that DCLK1 is absent from 63% of synapses. These results suggests that DCLK1 may not be involved in DCV transport in axons because DCLK1 co-localizes with 21 % of all axonal DCVs. However, it may still regulate movement of other KIF1A cargo, such as SVPs, at synaptic sites (Liu et al., 2012). A visual summary of the values obtained by MINER analysis of both sets of immunostained neurons is shown in figure 3-10. A summary of the raw data obtained from MINER analysis is shown in the appendix section (table A1 and table A2).













	<u>Synapse</u>	<u>Synapse</u>	<u>Synapsin and no chromogranin A</u>	<u>Transiting vesicle</u>
Reference Channel	Synapsin 	Synapsin 	Chromogranin A 	Chromogranin A 
Marker 1	Homer 	chromogranin A 	Synapsin 	Synapsin 
Marker 2	DCLK1 	DCLK1 	DCLK1 	DCLK1 
Frequency observed	61.1%	65.8%	18%	21%

Figure 3-11: Summary of results obtained from MINER analysis.

DCLK1 was absent from 61.1% of synapses where synapsin and Homer were co-localized. Similarly, DCLK1 was found to be absent from 65.8% of synapses where synapsin and chromogranin A co-localized. Taking these two measurements, DCLK1 was on average absent from 63.45% of all sites marked as synapses. MINER analysis also showed that DCLK1 co-localized with 21% of chromogranin A and 18% of synapsin.

Chapter 4.

Discussion

4.1. Summary

DCVs carry molecules, such as neuropeptides and neurotrophins, that are essential for synapse formation and maintenance. These vesicles can travel bidirectionally in the axon transported by KIF1A and dynein motors (Kwintar et al., 2009; Lo et al., 2011). DCV accumulation at synaptic sites is necessary for timely neuropeptide release via vesicle fusion upon excitation of a synapse (Guzik and Goldstein, 2004), therefore, regulated movement of DCVs is necessary for synaptic delivery of DCVs. Although some research observing DCV movement in other organisms had been done, DCV trafficking behaviour and the mechanism that allows for vesicle capture at synapses had not been previously studied in mammalian neurons.

As a prelude to characterizing synaptic capture, my research on DCV trafficking in hippocampal neurons confirmed bidirectional DCV movement and showed that there is no preferred direction for movement of axonal DCVs. Live imaging to track DCV movement demonstrated there was no significant difference between the number of anterograde and retrograde DCVs traveling along the axon. Furthermore, DCVs exhibited a similar movement behavior regardless of the direction they were traveling in; similar flux, run length, and velocities were observed in both directions. DCV tracking also showed that DCVs can undergo reversal and pausing events at different points in the axon. Furthermore, in addition to trafficking behavior, I also observed that DCVs can be captured at synaptic sites regardless of whether they are moving anterogradely or retrogradely. My DCV trafficking data suggest that DCVs in mammalian neurons follow a trafficking pattern similar to the one observed in *Drosophila* neurons.

Finally, to study the regulation of DCV capture at synapses, I focused on DCLK1, a MAP and KIF1A movement modulator. Specifically, I studied whether absence of DCLK1 from synapses could weaken the stability of the KIF1A-microtubule interaction at synapses and thereby lead to KIF1A pausing at synaptic sites allowing for DCV capture. To determine this, I measured co-localization of DCLK1 with DCVs and quantified presence of DCLK1 at synapses. My analysis showed that DCLK1 co-localized with a

small portion of axonal DCVs (21%). Furthermore, my co-localization analysis also showed that DCLK1 is absent from approximately two thirds of all synaptic sites (64%). Although a small percentage of axonal DCVs co-localize with DCLK1, it is possible that DCLK1 might regulate movement of other KIF1A cargo at synaptic sites.

4.2. Regulation of bidirectional DCV movement

Research carried out in *Drosophila* neurons describe DCVs axonal trafficking pattern as one resembling a “conveyor belt”. In this pattern, vesicles bypass the proximal *en passant* boutons and move towards the synapse to the distal end first; DCVs accumulate there and the vesicles not captured at this site then switch directions. DCVs then move retrogradely towards the cell body and start to fill the *en passant* boutons along the way; before entering the cell body, vesicles switch motors and move anterogradely again. This cycle repeats itself until all synapses are filled (Wong et al., 2012). To have a better understanding of the movement behavior of DCVs as they travel in the axon, and whether it resembles the one observed in *Drosophila*, my first aim was to quantify different parameters of DCV movement in axons of hippocampal rat neurons to better understand DCVs trafficking patterns.

My results confirmed bidirectional movement of DCVs in axons, as almost the same proportion of anterograde and retrograde events are observed (Figure 3-3A). Previous research in the Silverman laboratory had described similar bidirectional movement of DCVs (Kwintar et al., 2009). Furthermore, my data showed that both dynein and KIF1A-based transport exhibit similar behavior as DCVs moved along the axon. Both dynein and KIF1A moved at similar speeds, 1.87 $\mu\text{m/s}$ anterogradely and 1.86 $\mu\text{m/s}$ retrogradely (Figure 3-3C). Compared to other vesicles transported as part of the FAT system in the axon, DCVs move at a relatively high velocity. For example, autophagosomes move at a significantly lower speed, approximately 0.45 $\mu\text{m/s}$, compared to the DCV velocity observed in my data (Klinman and Holzbaur, 2016). Furthermore, although mitochondria move at varying speeds, they move at a peak velocity (1 $\mu\text{m/s}$; Klinman and Holzbaur, 2016) lower than the average DCV velocity seen in my research. There are only few FAT system organelles that can move faster than DCVs. Vesicles such as signaling endosomes and amyloid precursor protein (APP) can move at faster speeds than DCVs; signaling endosomes moves at speeds up to 3 $\mu\text{m/s}$

and APP at 2 $\mu\text{m/s}$ on average (Klinman and Holzbaur, 2016). Piccolo-Basoon vesicles (PTVs), small vesicles that transport architectural components of synapses, also move at speeds slightly higher than DCVs. PTVs move at approximately 2.03 $\mu\text{m/s}$ anterogradely and 2.8 $\mu\text{m/s}$ retrogradely (Fejtova et al., 2009).

My research also showed that DCVs also exhibited similar run lengths for both anterograde and retrograde movement (Figure 3-3D); a run length of 5 μm was observed for both directions of movement. These run lengths are within the range expected for KIF1A as per research performed in the Silverman laboratory before (Kwintar et al., 2009). Compared to run lengths of other FAT organelles, the motor proteins attached to DCVs exhibit longer run lengths. For example, on average, mitochondria run lengths are between 0.7 to 1.7 μm long (Narayanareddy et al., 2014), whereas in my research, the average length for anterograde runs was 5 μm . These extended run lengths observed in DCVs are the result of a specialized structure, the K loop, present in the DCV motor protein KIF1A that enhances binding of the motor protein to microtubules, and thus, prevents KIF1A from falling off the microtubule tracks (Siddiqui and Straube, 2017).

Because DCVs carry neurotrophins, necessary for synapse formation and maintenance, and neuropeptides, released during synaptic activity for cell signaling, a constant supply of DCVs is necessary in synaptic sites for synapse maintenance and function. The high trafficking velocity observed in my DCV data could be to ensure fast resupply of DCVs to newly emptied synaptic sites following activity. High trafficking velocities can be especially important for delivery of DCVs to the most distal synapses in mammalian neurons because of the large distances vesicles must travel between the cell body and the distal axon. Furthermore, having processive motors, capable of moving long distances before falling off the tracks, can be another way to ensure that DCVs reach the axon terminal and distal synaptic sites.

In addition to measuring different parameters of DCV movement, through kymograph analysis in my project, I observed that DCVs can undergo pausing and reversal events at different points in the axon (Figure 3-2). Research by the Holzbaur lab showed that the likelihood of vesicle pausing for SVPs and DCVs at synaptic sites is higher than at other points in the axons. This finding suggests that the pauses might act as a mechanism for vesicles to scout for potential capture sites (Guedes-Dias et al.,

2019). Furthermore, similar to my data, separate research by the Dean laboratory in mammalian neurons also observed DCV reversals, although most of the reversal events observed by this group occurred in the distal axon (Bharat et al., 2017). Differences in the location and number of reversal events I observed versus the data obtained by the Dean laboratory could be due to differences in the stage of maturation of the neurons used: my research was performed in 5 DIV neurons while the research in the Dean laboratory was performed in >13 DIV neurons. I observed that some DCVs switch directions in a short period of time during reversal events. These quick reversal events suggest that both motor proteins may already be attached to the vesicle. Instead cargo binding to one of the motor proteins, the direction of movement may therefore depend on motor activation, a description that fits the coordination model of bidirectional movement (Fu and Holzbaaur, 2014). My findings further support the idea that the coordination model can explain bidirectional DCV movement, although regulation of coordinated movement for DCVs is still unclear.

Research previously carried out in the Silverman laboratory showed that disruptions to dynactin caused a reduction in anterograde and retrograde movement. This observation suggested that dynactin can coordinate bidirectional DCV movement because it is necessary for both kinesin and dynein based transport (Kwintar et al., 2009). Furthermore, research studying the interaction between the carboxypeptidase E (CPE) tail, present in the DCV membrane, and dynactin proposed a mechanism by which bidirectional movement can be regulated. Interaction between CPE and dynactin allows for recruitment of either KIF1A or dynein, and thus can determine direction of movement depending on the motor protein attached to the DCV via dynactin (Park et al., 2008). Similarly, recent studies in *C. elegans* neurons found interactions between the N-terminal of P150 of dynactin, the intermediate chain of dynein, and the stalk of UNC-104 (Chen et al., 2019). This study indicates that the interaction between these subunits allows dynactin to regulate bidirectional movement of KIF1A cargoes, such as DCVs and SVPs, by binding both kinesin and dynein simultaneously. Depending on the conformation of the dynactin/dynein and KIF1A complex, either dynein or KIF1A is activated and can bind the microtubules and thus determine the direction of movement. Some of the reversal events seen in my kymograph analysis show that switches in direction can happen over a short period of time. This swift change in direction of movement could be explained by the coordination model involving dynactin explained

above because activation of one motor protein over the other one, rather than binding of either motor protein, would allow for these fast changes in direction.

In addition to coordination of bidirectional movement, research in *C. elegans* showed that interactions between UNC-104 and dynein may allow for motor pausing. Experiments tracking UNC-104 movement in dynactin/dynein mutants showed that absence of this complex resulted in a reduction in motor activity and processivity and an increase in the length of vesicle pausing and vesicle clustering (Chen et al., 2019). This study suggests the existence of a mechanism, called microtubule tethering, that regulates vesicle pausing by tethering the cargo to a microtubule while one of the motor proteins is inactive. When regulating UNC-104 movement, dynein is suggested to act as a tether while UNC-104 resumes movement. Based on these studies, interactions between UNC-104/KIF1A, dynein, and dynactin could explain the reversal and pausing events followed by resumed movement observed in my research. A mechanism that allows for fast changes in direction can be a way to ensure sufficient distribution of DCVs to sites where they are needed, as motor proteins would be able to deliver vesicles to sites from either direction.

Although the microtubule tethering model could explain reversal and pausing events in the axon, it is unclear if it is also involved in vesicle pausing specifically for capture events. Because I observed that vesicles can pause both inside and outside of synaptic sites, it is possible that there are different mechanisms that regulate temporary vesicle pausing, outside of synaptic sites, versus vesicle pausing that leads to vesicle capture at synaptic sites. Furthermore, research performed by the Holzbaur lab, showed that the likelihood of SVPs and DCVs pausing is higher near synapses (Guedes-Dias et al., 2019) which suggests that vesicle pausing near capture sites seems to increase the likelihood of capture for SVPs and potentially for DCVs. A mechanism that allows vesicles to temporarily pause but then resume movement would let vesicles scout potential capture sites, but still allow for constant vesicle supply to synapses. An increase in vesicle pausing specifically at synapses, due to accumulation of microtubules ends, has been proposed as one of the mechanisms that regulate pausing for vesicle capture at synapses (Yagensky et al., 2016), however, it is unclear how temporary pausing events are regulated. Overall, these observations highlight that regulation of KIF1A movement is key for delivery of both SVPs and DCVs to synaptic sites.

4.3. DCV capture at pre-synaptic sites

Synapse formation and maintenance depends on several steps that include vesicle synthesis, vesicle transport by a motor protein, pausing at a target site, and finally vesicle capture for later release (Chia et al., 2013). Because vesicle movement and capture are separate events, I also tracked DCVs as they approach synaptic sites for capture.

There are different parameters used to define vesicle capture. In *Drosophila* neurons, vesicles are considered captured when they remain stationary for a period of over five minutes (Wong et al., 2012). In contrast, in research with mammalian neurons, vesicles are considered captured when they become stationary for longer than two minutes (Bharat et al., 2017). To distinguish between pausing and capture events, I generated movies over three minutes long to track DCV movement. Based on the definition of capture in *Drosophila* neurons (Wong et al., 2012), I attempted to generate movies over five minutes long, however, due to photobleaching of the fluorescent tags attached to my DCV and SVP markers and phototoxicity, only movies up to four minutes long were successfully obtained. Using these movies and kymograph analysis, I defined DCV capture when previously moving DCVs became stationary for over three minutes at sites where there was accumulation of synaptophysin. This parameter was chosen to allow for a better distinction between temporarily paused vesicles versus captured ones, as stationary vesicles were seen to resume movement up to 120 seconds after pausing (Wong et al., 2012). Quantification of vesicles captured at these sites showed that although anterograde capture events were 1.5 times more frequent than retrograde events, there was no significant difference between the number of anterograde and retrograde events. (Table 3-1). Although I observed no statistically significant difference between the number of capture events, an anterograde bias in vesicle pausing at synaptic sites has been seen for the delivery of SVPs and DCVs to synaptic sites in mammalian neurons (Guedes-Dias et al., 2019). Furthermore, an anterograde bias in vesicle capture has been observed in *Drosophila* neurons following neuropeptide release during activity (Shakiryanova et al., 2006).

In addition to the experiments above, I attempted to confirm synaptic sites using different approaches. For one approach, I transfected neurons with BDNF-RFP and Syn-GFP and, after live-imaging, I stained them with FM 1-43FX dye

(ThermoFisher). This dye acts as a molecular probe to mark sites of vesicle fusion. Because DCVs and synaptic vesicles release their content at synapses via vesicle fusion, I used the dye to mark synaptic sites. However, despite several attempts and modifications to the standard protocol, the FM dye approach was unsuccessful as it was highly toxic and high background fluorescence. In a similar approach, I attempted to use anti-Homer as a post-synaptic marker to confirm synaptic sites. Neurons transfected with BDNF-RFP and Syn-GFP were stained with anti-Homer after live-imaging. Places of accumulation of stationary Syn-GFP and BDNF-RFP were expected to have a Homer partner. Despite successful Homer staining, the exact portion of the axon used for tracking of vesicle movement was rarely found and therefore no significant numbers of data were obtained. As an alternative to the approaches mentioned here, capture data was obtained from movies of at least three minutes long to study capture events.

In my DCV capture research, I observed capture of vesicles at synaptic sites regardless of the direction of travel. Similar to my results, research in *Drosophila* neurons showed that DCVs can be captured traveling in either direction and that there is no difference in the probability of cargo release via vesicle fusion between anterogradely and retrogradely captured DCVs. Furthermore, this research showed that both recently captured as well as stored vesicles have similar release probabilities (Wong et al., 2015). Taken together, my research and that performed in *Drosophila* suggest that regardless of the direction of travel, all DCVs that enter the axon may have undergone maturation steps, at either the cell body or at the proximal axonal segment, and are already fusion competent as they travel along the axon. This observation is supported by studies showing that a mechanism to prevent premature fusion of axonal DCVs, regulated by CaMKII, is needed in *C. elegans* because DCVs entering the axon are already mature and fusion competent (Hoover et al., 2014). Furthermore, these findings suggest that DCVs in the axon form a large pool of readily available mature vesicles. The existence of this pool could be advantageous to keep a constant supply of DCVs to synapses when needed. Because of the long distances DCVs must travel between the cell body and synaptic sites, bidirectional movement of mature vesicles would ensure an even distribution of vesicles in both the proximal and distal segments of the axon. Furthermore, by allowing vesicles to be captured in either direction, the chances of vesicle capture at synaptic sites are increased. Therefore, having a large population of mature vesicles ready for capture moving in both directions would allow for a faster and

steady supply of DCVs to synaptic sites and thus allow for a rapid response to synapse replenishment.

While working on this portion of my thesis project, other groups working on the same topic published papers describing movement of DCVs and SVPs, both KIF1A cargoes, in axons. Research in mammalian neurons carried out by the Dean laboratory described features of bidirectional movement of DCVs similar to the ones observed in my data and then studied regulation of DCV accumulation at synapses by regulation of motor-cargo interactions (Bharat et al., 2017). Furthermore, research done by the Holzbaur laboratory described SVP and DCV movement near synaptic sites. Their research using vesicle tracking in mammalian neurons showed that DCVs and SVPs move at similar speeds, exhibit similar run lengths and have increased pausing near synaptic sites (Guedes-Dias et al., 2019). Furthermore, both groups described two potential mechanisms that may regulate vesicle accumulation at synaptic sites.

These studies on the regulation of capture of KIF1A cargoes at synapses showed two potential mechanisms that could regulate this event. One mechanism indicates that regulation of DCV pausing and accumulation at synapses could be due to disruption of the cargo-motor interactions caused by phosphorylation of a DCV transmembrane protein, syt-4. Specifically, this study suggests that syt-4 phosphorylation, by the kinase JNK, at synaptic sites disrupts binding of DCVs to KIF1A, which then leads to vesicle drop-off and capture at synapses (Bharat et al., 2017). In contrast, another model suggests that vesicle pausing and accumulation at synapses is regulated by disruption of the motor-microtubule interactions. By tracking KIF1A movement, the Holzbaur laboratory showed that KIF1A runs stop at GTP-rich microtubule ends accumulated at synapses, thereby suggesting that vesicle capture occurs due to KIF1A pausing at synapses caused by impaired KIF1A-microtubule interactions (Guedes-Dias et al., 2019). My research on DCV capture at synapses supports the second model of regulation. Despite the anterograde bias observed in vesicle capture, vesicles moving retrogradely can still pause and be captured at synapses and therefore changes in microtubule structure would disrupt microtubule interactions for both KIF1A and dynein and thus it would allow either motor to pause near capture sites. Furthermore, the pausing events that do not lead to vesicle capture, could also be explained by this model as the result of momentary disruption between the motor protein, either KIF1A or dynein, and microtubule interactions. Although a

disruption in motor protein binding to microtubules explains regulated vesicle pausing, the signaling cascade involved in vesicle capture after vesicle pausing is still unclear.

4.4. Regulation of KIF1A movement near capture sites

Studies observing SVP and DCV behavior near synapses showed that vesicles traveling anterogradely, attached to KIF1A, are more likely to pause near synapses. KIF1A pausing near synapses appears to be essential to increase the likelihood of vesicle capture at these target sites (Guedes-Dias et al., 2019). Furthermore, it has been proposed that differences in microtubule structure near synaptic sites regulate KIF1A pausing for vesicle accumulation at synapses (Yagensky et al., 2016; Guedes-Dias et al., 2019). Because changes in microtubule structure may be important for motor pausing at synapses, regulated KIF1A movement could also be affected by localized MAPs distribution near synaptic sites. Previous research showed that DCLK1 can affect KIF1A movement by modifying motor-microtubule interactions (Liu et al., 2012), therefore, I focused on the role of DCLK1 at capture sites. As the next aim of my thesis, I used co-localization analysis to determine whether absence of DCLK1 near capture sites could regulate DCV pausing to increase the probability of capture at synaptic sites.

To define the parameters for quantification of vesicle co-localization, I used the size of pre-synaptic sites boutons (0.5 to 1.0 μm ; Ahmari and Smith, 2002) to establish the search radius for the co-localization analysis in MINER. After testing different search radii and measuring the distance between the puncta from the three markers, a distance of 300 nm was decided as the optimal search radius for my MINER analysis. The search radius of 300 nm was used to find near neighbour ROIs for the ROIs of the reference channel: synapsin was used as the reference channel for the first co-localization experiment and chromogranin A was the reference channel for the second co-localization experiment. This search radius was used to distinguish co-localized vesicles from adjacent ones. Using this co-localization parameter, I observed that 17% of DCVs and Synapsin vesicles co-localized (table 3-3). The low number of synapses found in my analysis can be explained by different factors, such as the low plating concentration of neurons and low number of interacting processes in the region that was sampled during imaging. Furthermore, recent research has shown that DCV fusion has a low probability release, only 1-6% of the total DCV pool undergo fusion, and

there is only a 30% chance of finding DCVs inside a synapse. The majority of DCVs appear to be away from the active zone in the periphery of the synapse (Persoon et al., 2018), which justifies my observations that most chromogranin puncta are observed outside of the pre-synaptic site. Finally, it is possible that the low percentage of co-localization between chromogranin A and synapsin would be increased by using a larger search radius. By using a modified version of a Sholl analysis, using an increasing large search radius and then categorizing the co-localized puncta by the distance between the ROIs, it would be possible to see if most chromogranin puncta is found outside of the synaptic sites.

Because DCLK1 affects DCV movement in dendrites (Lipka et al., 2016) and SVP transport in axons (Liu et al., 2012), I aimed to quantify the co-localization between DCVs and DCLK1 in axons. Co-localization of synapsin puncta with DCLK1 was also measured as a negative control. Although synapsin accumulates at synaptic sites, synapsin is part of the slow axonal transport system and it is not a KIF1A cargo (Tang et al., 2013), therefore, a low co-localization value between synapsin and DCLK1 was expected. Indeed, a low percentage of synapsin puncta co-localized with DCLK1 (18%). My co-localization analysis also showed that a small percentage of DCVs (21%) interact with DCLK1 in axons (Table 3-3). This result suggests that DCLK1 might not regulate axonal movement of DCVs. However, further experiments such as the ones described in section 4.5 are needed to determine whether DCLK1 interacts with KIF1A and if it has a direct impact on the movement of axonal DCVs.

Despite the low percentage of DCVs co-localized with DCLK1 observed in my research, DCLK1 regulates KIF1A-based transport of DCVs in dendrites (Lipka et al., 2016) and SVPs in axons (Liu et al., 2012). My data suggests that while DCLK1 may not regulate the majority of DCV transport in axons, it may still be involved in the regulation of axonal KIF1A movement when this motor is attached to a different cargo, i.e., SVPs. Examples in which attachment of specific cargo affect the behavior of a motor protein have previously been observed in other kinesins such as KIF5. This motor protein can move cargoes from both the slow and fast axonal transport systems, depending on the adaptor protein mediating cargo-motor interactions. For example, KIF5 transports mitochondria transport, a FAT cargo in neurons. Interaction between KIF5 and mitochondria is through the Miro/Milton complex and these adaptor proteins regulate KIF5's saltatory movement in mitochondria (Hirokawa et al., 2010). In contrast, when

KIF5 binds to neurofilaments through interactions between KLC and Hsc70, it moves in a pattern described observed in the slow axonal transport system (Hirokawa et al., 2010). The differences in KIF5 behavior depending on cargo binding using different adaptor proteins are an example of how specific cargo-motor interactions can regulate motor behavior.

Furthermore, if the interaction between KIF1A and DCLK1 depends on the cargo attached to the motor protein, it is possible that mechanisms, similar to the ones observed in KIF5, may also regulate KIF1A transport behavior. For example, it is possible that differences in motor-cargo interaction between SVPs, DCVs, and KIF1A may also be responsible for selective transport of cargoes into axons and dendrites. Again, KIF5 provides an example of a motor protein that exhibits different trafficking behaviors depending on the cargo and the adaptor proteins bound to the motor. In mammalian neurons, KIF5 interaction with TRAK1, a Milton mammalian homologue localized mostly in axons, guides movement of mitochondria into axons. In contrast, KIF5 interaction with TRAK2, localized mostly in dendrites, guides mitochondria movement into dendrites (Melkov and Abdu, 2018). It is possible that differences in adaptor proteins regulating binding of DCVs and KIF1A, versus SVPs and KIF1A, might also regulate other aspects of motor behavior.

Quantification of DCLK1 at synaptic sites using MINER analysis showed that DCLK1 is absent from 64% of synapses (Table 3-3). Although DCLK1 is not absent from all synapses, presence of DCLK1 at some synaptic sites (36%) can be justified. Because microtubules can be continuous underneath synapses, it is possible that the DCLK1 observed at some synaptic sites is on microtubules that allow for vesicle movement beyond the synaptic sites. Vesicle pausing is important for capture, however, vesicles also need to move past proximal synaptic sites to reach distal ones. If DCLK1 was entirely absent from synaptic sites, KIF1A movement might be disrupted, as it would not move beyond pausing sites, and therefore vesicle supply to distal synapses would be reduced. DCLK1 is necessary for axonal SVP transport (Liu et al., 2012), therefore, it is possible that DCLK1 is present in some synapses to allow for sufficient SVP supply to distal synaptic sites and the axon terminal. Further MINER analyses, such as the one described in section 4.5, are needed to quantify whether the distribution of DCLK1 in axons is random or follows a specific pattern.

Because binding of DCLK1 to microtubules is regulated, it is possible that the percentage of DCLK1 co-localized at synaptic sites might be due to a mechanism that decreases the interaction between DCLK1 and microtubules at synapses. Interaction of microtubules and DCX proteins, including DCLK1, depends on phosphorylation of serine residues at the microtubule binding domains by several kinases, such as CDK5, PKA, and JNK1 (Ramkumar et al., 2018). Specifically, phosphorylation of these serine residues lowers microtubule binding affinity. Because DCLK1 binding to microtubules depends on phosphorylation, it is possible that the absence of DCLK1 from two-thirds of synapses observed in my co-localization analysis might be due to phosphorylation of the microtubule-binding domain of DCLK1 by kinases, such as CDK5 or JNK1, that might be concentrated at synaptic sites.

Overall, DCV transport and pausing appears to be regulated by multiple coordinated mechanisms to ensure correct DCV distribution in neurons. Precise DCV trafficking is necessary for the well-being and survival of organisms because absence of DCVs at synaptic sites, caused by either faulty motor movement or lack of vesicle accumulation, has severe detrimental effects. For example, decrease in BDNF levels has been linked to neurodegenerative diseases such as Huntington's disease as well as Alzheimer's. Research tracking BDNF levels in cortical neurons showed that a decrease in BDNF release, caused by alterations to vesicle trafficking, was observed in cortical neurons obtained from Huntington's disease mouse models (Yu et al., 2018). In addition to Huntington's disease, reduced levels of BDNF due to alterations in vesicle trafficking have been associated with Alzheimer's diseases. Studies in hippocampal neurons showed that impaired anterograde and retrograde transport of BDNF vesicles, due to APP overexpression, was observed in Alzheimer's disease mouse models (Seifert et al., 2016). Furthermore, several neurodegenerative diseases linked to mutations in KIF1A, the DCV and SVP anterograde motor protein, highlight the importance of correct motor protein movement for whole organism survival. For example, sequencing studies in samples obtained from patients with encephalopathy and brain atrophy showed that these patients had de novo mutations in the motor binding domain of KIF1A (Lee et al., 2015). Finally, studies of UNC-104, a KIF1A homologue in *C. elegans*, showed that reduced levels of active UNC-104 is present in aged animals. A decrease in UNC-104 levels causes a reduction in movement of vesicles transported by this motor, which may be responsible for some of the age-associated synapse defects (Li et al., 2016).

4.5. Conclusion and future perspectives

In conclusion, my research provides more information about DCV trafficking behavior as they travel in the axon and approach synaptic sites. My data on DCV bidirectional movement emphasizes the importance of motor protein regulation, of both KIF1A and dynein, in vesicle supply to synaptic sites. Furthermore, my co-localization analysis further supports the idea that differences in microtubule structure near synapses could act as local cues that regulate vesicle pausing, and therefore, affect vesicle capture and accumulation. Ultimately, my research highlights the importance of transport mechanisms as they directly support synaptic development and overall neuronal function.

My experiments studying DCV trafficking behavior were done in spontaneously active mammalian neurons, therefore more experiments to see if DCV behavior is the same following neuropeptide release during induced synaptic activity are required. Studies in *Drosophila* neurons observed a change in DCV trafficking patterns after neuropeptide release; more retrograde DCVs were captured to synaptic sites after activity (Shakiryanova et al., 2006). This increase in retrograde capture observed in *Drosophila* neurons may allow for a more timely resupply of DCVs to sites where DCV accumulation is reduced due to vesicle fusion for neuropeptide release. Because DCVs need to travel longer distances between the cell body and distal synaptic sites, an increase in retrograde capture would explain how a constant supply of DCVs to synapses is maintained even at distal synaptic sites. To have a better understanding of DCV behavior at synaptic sites, studies measuring whether the same changes in DCV trafficking pattern observed in *Drosophila* neurons after depolarization also occur in mammalian neurons should be performed similarly to the experiments described herein.

Furthermore, the reversal and pausing events shown in my data emphasize the importance of understanding the regulation of bidirectional movement in DCVs. Because recent studies in *C. elegans* showed that the interaction between specific subunits of dynactin, dynein, and UNC-104 may regulate bidirectional movement and pausing (Chen et al., 2019), more research studying KIF1A interactions with the dynactin/dynein complex are needed. KIF1A, dynactin, and dynein interact via the CPE tail in DCV membranes in mammalian neurons (Park et al., 2008), however, whether the same interaction between specific subunits recently observed in *C. elegans* are present in

mammalian neurons should be confirmed. Specifically, whether simultaneous binding between dynactin, KIF1A, and dynein can be observed in mammalian neurons as well. Furthermore, studies tracking the effect of dynactin/dynein knockdown on DCVs reversals and pausing would further determine whether this complex is in charge of coordinating bidirectional movement of DCVs in mammalian neurons. Because the interaction between UNC-104 and dynactin/dynein may also affect vesicle pausing, knockout studies would also help determine whether the “microtubule tethering” model is also involved in DCV pausing at capture sites.

The role of DCLK1 for trafficking of other KIF1A cargoes, such as SVPs, has been previously shown (Liu et al., 2012) . Based on this previous research, despite low co-localization between axonal DCVs and DCLK1 in my data, co-localization between DCLK1 and other KIF1A cargoes, such as synaptophysin vesicles, should be quantified. If a high percentage of co-localization between DCLK1 and axonal SVPs is observed, it would indicate a difference in KIF1A behavior depending on the type of cargo bound to the motor. If co-localization between SVPs and DCLK1 is confirmed, immunoprecipitation analysis would help determine whether interactions with an adaptor protein regulating DCVs, but not SVPs, binding may either block or cause steric hindrance at the interaction site between KIF1A and DCLK1. Differences in motor protein behavior due to interactions with an adaptor proteins have been observed in other kinesins, such as KIF5 (Hirokawa et al., 2010), therefore it is possible that cargo-specific adaptor proteins regulate the difference in KIF1A interaction with DCLK1 as well as regulate selective transport. Ultimately, these experiments would help determine whether there are differences in the interaction between KIF1A and DCLK1 depending on the cargo bound to the motor protein.

To determine whether the value obtained for co-localization of DCLK1 at synaptic sites is statistically significant, further MINER analyses should be performed. By performing multiple MINER analyses, while increasing the search radii by a constant distance each time, it would be possible to quantify whether the likelihood of finding DCLK1 at synaptic sites is more or less than the likelihood of finding DCLK1 at any other points in the axon. These data would confirm whether absence of DCLK1 at synaptic sites is a regulated event or if it happens by chance. Finally, in addition to further MINER analysis, studies using DCLK1 knockdowns, or gain-of-function mutants, would also be needed. These studies would be useful to determine whether DCLK1 has a direct effect

on axonal movement of DCVs and SVPs and to determine whether DCLK1 regulates SVP or DCV capture at synapses.

Finally, absence of DCLK1 from synapses would indicate that binding of DCLK1 to microtubules at synaptic sites is an event regulated by a mechanism that either allows or impairs DCLK1 binding to microtubules specifically at these sites. DCLK1 binding to microtubules can be regulated by phosphorylation of the microtubule-binding domains by kinases such as JNK1 or CDK5 (Ramkumar et al., 2018). An experiment to determine whether these kinases are more concentrated, or more active, at synaptic sites would determine whether they might regulate DCLK1 binding to microtubules at synapses specifically. Furthermore, by observing the effect of generating a DCLK1 plasmid with a point mutation that impairs the phosphorylation of the microtubule binding domain of DCLK1, it would be possible to assess whether presence of DCLK1 at synaptic sites is regulated by phosphorylation and could also be used to assess whether increased presence of DCLK1 at synapses affects vesicle accumulation.

Overall, a better understanding of regulation of DCV movement in axons could be useful to give new insights into the mechanisms that help define synapse plasticity and neuronal function. These mechanisms could then also be used to better understand the role of organelle trafficking in neurodegenerative diseases such as Alzheimer's and Huntington's disease.

References

- Allredge B (2010) Pathogenic involvement of neuropeptides in anxiety and depression. *Neuropeptides* 44:215–224.
- Atherton J, Houdusse A, Moores C (2013) MAPping out distribution routes for kinesin couriers. *Biol Cell* 105:n/a-n/a.
- Bharat V, Siebrecht M, Burk K, Ahmed S, Reissner C, Kohansal-Nodehi M, Steubler V, Zweckstetter M, Ting JT, Dean C (2017a) Capture of Dense Core Vesicles at Synapses by JNK-Dependent Phosphorylation of Synaptotagmin-4. *Cell Rep* 21:2118–2133.
- Bharat V, Siebrecht M, Burk K, Ahmed S, Reissner C, Kohansal-Nodehi M, Steubler V, Zweckstetter M, Ting JT, Dean C (2017b) Capture of Dense Core Vesicles at Synapses by JNK-Dependent Phosphorylation of Synaptotagmin-4. *Cell Rep* 21:2118–2133.
- Burack MA, Silverman MA, Banker G (2000) The Role of Selective Transport in Neuronal Protein Sorting. *Neuron* 26:465–472.
- Bury LAD, Sabo SL (2016) Building a Terminal. *Neurosci* 22:372–391.
- Chen C, Peng Y, Yen Y, Bhan P, Muthaiyan Shanmugam M, Klopfenstein DR, Wagner OI (2019) Insights on UNC-104-dynein/dynactin interactions and their implications on axonal transport in *Caenorhabditis elegans*. *J Neurosci Res* 97:185–201.
- Chevalier-Larsen E, Holzbaur ELF (2006) Axonal transport and neurodegenerative disease. *Biochim Biophys Acta - Mol Basis Dis* 1762:1094–1108.
- Chia PH, Li P, Shen K (2013) Cell biology in neuroscience: cellular and molecular mechanisms underlying presynapse formation. *J Cell Biol* 203:11–22.
- Dehmelt L, Halpain S (2005) The MAP2/Tau family of microtubule-associated proteins. *Genome Biol* 6:204.

- Fejtova A, Davydova D, Bischof F, Lazarevic V, Altmann WD, Romorini S, Schöne C, Zuschratter W, Kreutz MR, Garner CC, Ziv NE, Gundelfinger ED (2009) Dynein light chain regulates axonal trafficking and synaptic levels of Bassoon. *J Cell Biol* 185:341–355.
- Franker MAM, Hoogenraad CC (2013) Microtubule-based transport - basic mechanisms, traffic rules and role in neurological pathogenesis. *J Cell Sci* 126:2319–2329.
- Fu M, Holzbaur ELF (2014) Integrated regulation of motor-driven organelle transport by scaffolding proteins. *Trends Cell Biol* 24:564–574.
- Goldstein AY, Wang X, Schwarz TL (2008) Axonal transport and the delivery of pre-synaptic components. *Curr Opin Neurobiol* 18:495–503.
- Gondré-Lewis MC, Park JJ, Loh YP (2012) Cellular Mechanisms for the Biogenesis and Transport of Synaptic and Dense-Core Vesicles. *Int Rev Cell Mol Biol* 299:27–115.
- Gross SP, Welte MA, Block SM, Wieschaus EF (2002) Coordination of opposite-polarity microtubule motors. *J Cell Biol* 156:715–724.
- Guedes-Dias P, Nirschl JJ, Abreu N, Tokito MK, Janke C, Magiera MM, Holzbaur ELF (2019) Kinesin-3 Responds to Local Microtubule Dynamics to Target Synaptic Cargo Delivery to the Presynapse. *Curr Biol* 29:268-282.e8.
- Guillaud L, Wong R, Hirokawa N (2008) Disruption of KIF17–Mint1 interaction by CaMKII-dependent phosphorylation: a molecular model of kinesin–cargo release. *Nat Cell Biol* 10:19–29.
- Guzik BW, Goldstein LS (2004) Microtubule-dependent transport in neurons: steps towards an understanding of regulation, function and dysfunction. *Curr Opin Cell Biol* 16:443–450.
- Hirokawa N (1998) Kinesin and dynein superfamily proteins and the mechanism of organelle transport. *Science* 279:519–526.
- Hirokawa N, Nitta R, Okada Y (2009) The mechanisms of kinesin motor motility: lessons from the monomeric motor KIF1A. *Nat Rev Mol Cell Biol* 10:877–884.

- Hirokawa N, Niwa S, Tanaka Y (2010) Molecular Motors in Neurons: Transport Mechanisms and Roles in Brain Function, Development, and Disease. *Neuron* 68:610–638.
- Hirokawa N, Noda Y, Tanaka Y, Niwa S (2009) Kinesin superfamily motor proteins and intracellular transport. *Nat Rev Mol Cell Biol* 10:682–696.
- Hirokawa N, Takemura R (2005) Molecular motors and mechanisms of directional transport in neurons. *Nat Rev Neurosci* 6:201–214.
- Hoover CM, Edwards SL, Yu S, Kittelmann M, Richmond JE, Eimer S, Yorks RM, Miller KG (2014) A novel CaM kinase II pathway controls the location of neuropeptide release from *Caenorhabditis elegans* motor neurons. *Genetics* 196:745–765.
- Jeong S (2017) Molecular and Cellular Basis of Neurodegeneration in Alzheimer's Disease. *Mol Cells* 40:613–620.
- Kaech S, Banker G (2006) Culturing hippocampal neurons. *Nat Protoc* 1:2406–2415.
- Kapitein LC, Hoogenraad CC (2011) Which way to go? Cytoskeletal organization and polarized transport in neurons. *Mol Cell Neurosci* 46:9–20.
- Klinman E, Holzbaur ELF (2016) Comparative analysis of axonal transport markers in primary mammalian neurons. *Methods Cell Biol* 131:409–424.
- Kwinter DM, Lo K, Mafi P, Silverman MA (2009) Dynactin regulates bidirectional transport of dense-core vesicles in the axon and dendrites of cultured hippocampal neurons. *Neuroscience* 162:1001–1010.
- Ligon LA, Steward O (2000) Movement of mitochondria in the axons and dendrites of cultured hippocampal neurons. *J Comp Neurol* 427:340–350.
- Lipka J, Kapitein LC, Jaworski J, Hoogenraad CC (2016) Microtubule-binding protein doublecortin-like kinase 1 (DCLK1) guides kinesin-3-mediated cargo transport to dendrites. *EMBO J* 35:302–318.

- Liu JS, Schubert CR, Fu X, Fourniol FJ, Jaiswal JK, Houdusse A, Stultz CM, Moores CA, Walsh CA (2012a) Molecular basis for specific regulation of neuronal kinesin-3 motors by doublecortin family proteins. *Mol Cell* 47:707–721.
- Luján R, Shigemoto R, López-Bendito G (2005) Glutamate and GABA receptor signalling in the developing brain. *Neuroscience* 130:567–580.
- Maday S, Twelvetrees AE, Moughamian AJ, Holzbaur ELF (2014) Axonal transport: cargo-specific mechanisms of motility and regulation. *Neuron* 84:292–309.
- Mojard Kalkhoran S, Chow SHJ, Walia JS, Gershon C, Saraev N, Kim B, Poburko D (2019) VNUT and VMAT2 segregate within sympathetic varicosities and localize near preferred Cav2 isoforms in the rat tail artery. *Am J Physiol Circ Physiol* 316:H89–H105.
- Moughamian AJ, Holzbaur ELF (2012) Synaptic vesicle distribution by conveyor belt. *Cell* 148:849–851.
- Nakata T, Hirokawa N (2003) Microtubules provide directional cues for polarized axonal transport through interaction with kinesin motor head. *J Cell Biol* 162:1045–1055.
- Narayanareddy BRJ, Vartiainen S, Hariri N, O'Dowd DK, Gross SP (2014) A biophysical analysis of mitochondrial movement: differences between transport in neuronal cell bodies versus processes. *Traffic* 15:762–771.
- Numakawa T, Odaka H, Adachi N (2018) Actions of Brain-Derived Neurotrophin Factor in the Neurogenesis and Neuronal Function, and Its Involvement in the Pathophysiology of Brain Diseases. *Int J Mol Sci* 19.
- Okada Y, Yamazaki H, Sekine-Aizawa Y, Hirokawa N (1995) The Neuron-Specific Kinesin Superfamily Protein KIF1A Is a Unique Monomeric Motor for Anterograde Axonal Transport of Synaptic Vesicle Precursors.
- Park JJ, Cawley NX, Loh YP (2008) A bi-directional carboxypeptidase E-driven transport mechanism controls BDNF vesicle homeostasis in hippocampal neurons. *Mol Cell Neurosci* 39:63–73.

- Park JJ, Koshimizu H, Loh YP (2009) Biogenesis and Transport of Secretory Granules to Release Site in Neuroendocrine Cells. *J Mol Neurosci* 37:151–159.
- Peled ES, Newman ZL, Isacoff EY (2014) Evoked and spontaneous transmission favored by distinct sets of synapses. *Curr Biol* 24:484–493.
- Ramkumar A, Jong BY, Ori-McKenney KM (2018) ReMAPping the microtubule landscape: How phosphorylation dictates the activities of microtubule-associated proteins. *Dev Dyn* 247:138–155.
- Rikitake Y, Takai Y (2008) Interactions of the cell adhesion molecule nectin with transmembrane and peripheral membrane proteins for pleiotropic functions. *Cell Mol Life Sci* 65:253–263.
- Rueden CT, Schindelin J, Hiner MC, DeZonia BE, Walter AE, Arena ET, Eliceiri KW (2017) ImageJ2: ImageJ for the next generation of scientific image data. *BMC Bioinformatics* 18:529.
- Shakiryanova D, Tully A, Levitan ES (2006) Activity-dependent synaptic capture of transiting peptidergic vesicles. *Nat Neurosci* 9:896–900.
- Siddiqui N, Straube A (2017) Intracellular cargo transport by kinesin-3 motors. *Biochem* 82:803–815.
- Tang Y, Scott D, Das U, Gitler D, Ganguly A, Roy S (2013) Fast vesicle transport is required for the slow axonal transport of synapsin. *J Neurosci* 33:15362–15375.
- van den Pol AN (2012) Neuropeptide transmission in brain circuits. *Neuron* 76:98–115.
- Venkatramani A, Panda D (2019) Regulation of neuronal microtubule dynamics by tau: Implications for tauopathies. *Int J Biol Macromol* 133:473–483.
- Wong MY, Cavolo SL, Levitan ES (2015) Synaptic neuropeptide release by dynamin-dependent partial release from circulating vesicles. *Mol Biol Cell* 26:2466–2474.
- Wong MY, Zhou C, Shakiryanova D, Lloyd TE, Deitcher DL, Levitan ES (2012) Neuropeptide delivery to synapses by long-range vesicle circulation and sporadic capture. *Cell* 148:1029–1038.

Yagensky O, Kalantary Dehaghi T, Chua JJE (2016) The Roles of Microtubule-Based Transport at Presynaptic Nerve Terminals. *Front Synaptic Neurosci* 8:3.

Yuan A, Rao M V, Veeranna, Nixon RA (2017) Neurofilaments and Neurofilament Proteins in Health and Disease. *Cold Spring Harb Perspect Biol* 9.

Appendix A

Table A1. Summary of MINER analysis for neurons stained with synapsin, Homer and DCLK1

		% co-localization
Synapsin ROIs analyzed	3270	-----
Number of Homer ROIs	2500	-----
Number of DCLK1 ROIs	4629	-----
Synapsin ROIs with NN	628	19.20
Homer partners for synapsin	54	1.65
DCLK1 partners for synapsin	594	18.17
Both Homer and DCLK1 Partners for synapsin	21	0.64

ROIs were generated from 18 neurons obtained from three different cultures

Table A2. Summary of MINER analysis for neurons stained with chromogranin A, synapsin and DCLK1

		% co-localization
Chromogranin A ROIs analyzed	3887	-----
Number of synapsin ROIs	3952	-----
Number of DCLK1 ROIs	4814	-----
Chromogranin A ROIs with a partner	1531	39.39
Synapsin partners for chromogranin A	690	17.75
DCLK1 partners for chromogranin A	841	21.64
Both synapsin and DCLK1 for chromogranin A	236	6.07

ROIs were generated from 20 neurons obtained from two different cultures